TITLE PAGE

Development of a high-resolution emission inventory and its evaluation and application through air quality modeling for Jiangsu Province, China

Yaduan Zhou[1], Yu Zhao[1,2*], Pan Mao[1], Qiang Zhang[3], Jie Zhang[2,4], Liping Qiu[1], Yang Yang[1]

1. State Key Laboratory of Pollution Control & Resource Reuse and School of the Environment, Nanjing University, 163 Xianlin Ave., Nanjing, Jiangsu 210023, China

2. Jiangsu Collaborative Innovation Center of Atmospheric Environment and Equipment Technology (CICAEET), Nanjing University of Information Science & Technology, Jiangsu 210044, China

3. Ministry of Education Key Laboratory for Earth System Modeling, Center for Earth System Science, Tsinghua University, Beijing 100084, China

4. Jiangsu Provincial Academy of Environmental Science, 176 North Jiangdong Rd., Nanjing, Jiangsu 210036, China

*Corresponding author: Yu Zhao

Phone: 86-25-89680650; email: *yuzhao@nju.edu.cn*

ABSTRACT

Improved emission inventories combining detailed source information are crucial for better understanding the atmospheric chemistry and effectively making emission control policies using air quality simulation, particularly at regional or local scales. With the downscaled inventories directly applied, chemical transport model might not be able to reproduce the authentic evolution of atmospheric pollution processes at small spatial scales. Using the bottom-up approach, a high-resolution emission inventory was developed for Jiangsu China, including SO_2, NOx, CO, NH_3, volatile organic compounds (VOCs), total suspended particulates (TSP), PM_{10}, $PM_{2.5}$, black carbon (BC), organic carbon (OC), and CO_2. The key parameters relevant to emission estimation for over 6000 industrial sources were investigated, compiled and revised at plant level based on various data sources and on-site survey. As a result, the emission fractions of point sources were significantly elevated for most species. The improvement of this provincial inventory was evaluated through comparisons with other inventories at larger spatial scales, using satellite observation and air quality modeling. Compared to the downscaled Multi-resolution Emission Inventory for China (MEIC), the spatial distribution of NO_X emissions in our provincial inventory was more consistent with summer tropospheric NO_2 VCDs observed from OMI, particularly for the grids with moderate emission levels, implying the improved emission estimation for small and medium industrial plants by this work. Three inventories (national, regional, and provincial by this work) were applied in the Models-3/Community Multi-scale Air Quality (CMAQ) system for southern Jiangsu October 2012, to evaluate the model performances with different emission inputs. The best agreement between available ground observation and simulation was found when the provincial inventory was applied, indicated by the smallest normalized mean bias (NMB) and normalized mean errors (NME) for all the concerned species SO_2, NO_2, O_3 and $PM_{2.5}$. The result thus implied the advantage of improved emission inventory at local scale for high resolution air quality modeling. Under the unfavorable meteorology in which horizontal and vertical movement of atmosphere was limited, the simulated SO_2 concentrations at downtown Nanjing (the capital city of Jiangsu) using the regional or national inventories were much higher than observation, implying the

overestimated urban emissions when economy or population densities were applied to downscale or allocate the emissions. With more accurate spatial distribution of emissions at city level, the simulated concentrations using the provincial inventory were much closer to observation. Sensitivity analysis of $PM_{2.5}$ and O_3 formation was conducted using the improved provincial inventory through the Brute Force method. Iron & steel and cement plants were identified as important contributors to the $PM_{2.5}$ concentrations in Nanjing. The O_3 formation was VOCs-limited in southern Jiangsu, and the concentrations were negatively correlated with NO_X emissions in urban areas owing to the accumulated NOx from transportation. More evaluations are further suggested for the impacts of speciation and temporal and vertical distribution of emissions on air quality modeling at regional or local scales in China.

1 INTRODUCTION

With rapid development of economy and growth of energy consumption, eastern China is experiencing severe atmospheric pollution attributed to the large emissions of primary air pollutants and the subsequent formation of secondary pollution, e.g., fine particles and O_3. Relatively high concentrations of surface $PM_{2.5}$ were observed in eastern China based on the national monitoring network (data source: http://106.37.208.233/), and only 9.5% out of 190 cities with the measurement data reported in 2014 met the National Ambient Air Quality Standard (NAAQS), i.e., 35 $\mu g/m^3$ for annual $PM_{2.5}$ concentration (MEP, 2012). Under the serious case of air pollution, series of measures have been conducted to reduce the pollutant emissions and to improve the air quality across the country. For example, the National Air Pollution Prevention Action Plan issued in 2013 required strict emission controls on both industry and transportation sectors, and aimed to achieve a 25%, 20% and 15% reduction of annual $PM_{2.5}$ concentration for Beijing-Tianjin-Hebei (JJJ), Yangtze River Delta (YRD), and Pearl River Delta (PRD) region from 2012 to 2017, respectively. Given the non-linear response of ambient concentrations to emissions, chemical transport modeling (CTM) has been widely applied to study the mechanisms of complex pollution processes and the impacts of emission abatement (Zhang et al., 2006; Streets et al., 2007; B. Zhao et al., 2013; Zhang et

al., 2012). As the key input of CTM, therefore, improved emission inventories, particularly at regional or local scales, become important for scientific air quality simulation and effective policy making.

Progress has been increasingly achieved in emission inventory studies for China. Compared to earlier national emission inventories including those for Transport and Chemical Evolution over the Pacific Mission (TRACE-P, Streets et al., 2003), Intercontinental Chemical Transport Experiment-Phase B (INTEX-B, Zhang et al., 2009), and Regional Emission inventory in Asia (REAS, Ohara et al., 2007; Kurokawa et al., 2013), Tsinghua University developed the Multi-resolution Emission Inventory for China (MEIC, http://www.meicmodel.org/), in which the information of large power plants and cement factories was investigated and the uncertainties of emission estimation for those typical sources were reduced (Wang et al., 2014). Besides, high-resolution emission inventories at regional and city scales were gradually established in the developed regions JJJ, YRD and PRD, attributed to better data support and stronger need to combat air pollution (Zheng et al., 2009; S. Wang et al., 2010; Huang et al., 2011; B. Zhao et al., 2012; Zhao et al., 2015).

Resulting from various methods and data sources, clear discrepancies exist in different emission inventories in China, both at national (Y. Zhao et al., 2013; Xia et al., 2016) and local scales (Zhao et al., 2015). When applied in CTM, the uncertainties in emission estimation would inevitably lead to bias in air quality simulation, besides the errors of meteorological field modeling and deficiencies of built-in atmospheric chemical mechanisms (Zheng et al., 2012). Based on the Models-3/Community Multi-scale Air Quality (CMAQ) system, for example, Zhang et al. (2014) simulated $PM_{2.5}$ and O_3 concentrations in southeastern United States using the different versions of national emission inventory (NEI), and compared the results with several ground observational datasets. The model performance with updated inventory (NEI05) was much better than that with old one (NEI99), indicating the impacts of emission inventory on the accuracy of CMAQ simulations. Han et al. (2015) conducted NO_2 vertical column simulation for China with CMAQ, and found that the modeled results using INTEX-B inventory were closer to satellite observation than those using REAS. At regional or local scales, emission inventory that incorporates the detailed information of individual sources is assumed to have advantages in air quality research prior

to downscaled national inventory that generally applied regional average levels of emission factors due to unavailability of data (Zhao et al., 2015). The benefits of improved emission estimation, spatial and temporal distribution, or chemical speciation of pollutants, however, have not been sufficiently confirmed with CTM. Recently, Yin et al. (2015) conducted CMAQ simulation on O_3 using updated VOC emission inventory for PRD, implying that the reduced uncertainties of total emission estimation and spatial distribution could improve the model performance compared with ground observation.

We select Jiangsu, a typical province with well-developed industry in eastern China, to develop and evaluate the high-resolution emission inventory. The geographic location and cities of the province are illustrated in Figure S1 in the supplement. With a total area of 107 200 km^2 and population of 79.2 million in 2012, Jiangsu was the first ranked province in gross domestic product (GDP) per capita in China (NBSC, 2013a; JSNBS, 2013). It accounted for 8.0%, 7.6%, 8.9%, and 10.2% of the country's power generation, cement, pig iron, and crude steel production in 2012, respectively (NBSC, 2013b). Intensive energy consumption and industry resulted in heavy air pollution: all the 13 cities had their annual average concentrations of $PM_{2.5}$ exceeding the NAAQS in 2012, with the highest reaching 74 $\mu g/m^3$ in the capital city, Nanjing. Clear uncertainties exist in current multi-scale emission inventories. Zhao et al. (2015), for example, estimated Nanjing's SO_2 and $PM_{2.5}$ emissions at 165 and 71 Gg in 2012, respectively, while the results by Fu et al. (2013) were 131.8 and 35.3 Gg. implying the necessity of improvement and assessment of regional emission inventory, for both scientific and policy implication. In this work, a comprehensive emission inventory for Jiangsu with high temporal and spatial resolutions was first established with the best available data of local emission sources incorporated. This provincial emission inventory was then compared with other inventories and satellite observation to test its improvement on emission estimation and spatial distribution. CMAQ was further applied to indicate the advantage of the provincial inventory prior to downscaled national and regional ones. In particular, the impacts of spatial distribution of emissions on model performance were analyzed for period with unfavorable meteorological condition. Finally, the improved inventory was applied for sensitivity analysis on regional $PM_{2.5}$ and O_3 formation.

2 DATA AND METHODS

2.1 Methodology of provincial emission inventory development

The emissions of gaseous pollutants (SO_2, NOx, CO, NH_3 and VOCs), greenhouse gas CO_2, particulate matter (total suspended particulates, TSP, PM_{10} and $PM_{2.5}$) and its chemical compositions (black carbon, BC and organic carbon, OC) of anthropogenic origin in Jiangsu were estimated with a bottom-up method. Emission sources were classified into seven main categories, including power plant, industry, solvent use, transportation, residential & commercial, agriculture and other sources. Industry was subdivided into iron & steel, cement, and other industry including nonferrous metal smelting, brick and lime kilns, chemical industry and other industry boilers. Residential & commercial sector included household combustion of fossil fuel and biofuel. Agriculture included livestock and fertilizer usage. Open biomass burning, cooking, and waste (water) disposal, were considered as other sources. The detailed categories were summarized in Table S1 in the supplement. For each category, point, mobile and area sources were defined depending on the detailed levels of information and the emission characteristics. For point sources, information on emission factor and activity level was investigated and compiled for individual plants, and the annual emissions of atmospheric pollutants were calculated using Eq. (1), as described in Zhao et al (2015).

$$E_i = \sum_{j,m} AL_{i,j,m} \times EF_{i,j,m} \times (1 - \eta_{i,j,m}) \quad (1)$$

where i, j and m represented the pollutant species, individual plant, and fuel/technology type, respectively; AL was the activity level data; EF was the uncontrolled emission factor; and η was removal efficiency of air pollutant control device.

Regarded as mobile sources, the emissions of on-road transportation were calculated by the CORPERT model (EEA, 2012) and then spatially allocated based on the road net information of the province. Area sources included non-road transportation, solvent use, residential & commercial sector, agriculture, and small industry plants without detailed information collected. The emissions from non-road transportation and agriculture were estimated following the methods by Zhang et al. (2010) and Dong et al. (2009), respectively. For other sources, the emissions were calculated using Eq. (2)

$$E_{i,n} = \sum_{m} AL_{i,m,n} \times EF_{i,m,n} \times (1 - \eta_{i,m,n}) \quad (2)$$

where n represented the source type; EF_n *and* η_n were the average levels of uncontrolled emission factors and removal efficiencies for given source n. For sources without any emission control measure (e.g., residential combustion), η=0.

2.2 Activity level

The main sources of activity data are summarized by category in Table S1 in the supplement. Most of coals in Jiangsu were used by power and industry sectors, and household accounted for only 0.3% of total coal consumption in the province in 2012 (JSNBS, 2013), indicating the significance to reduce the uncertainties of emission estimation for power and industry plants. Therefore a comprehensive database for power and industrial sector was established with the information collected and modified from the official environmental statistics, Pollution Source Census (PSC, internal data), and on-site survey on large emitters. Parameters including geographical location, combustion/production technology, fuel/burner/boiler type, installed air pollution control device (APCD) and its removal efficiency were investigated for individual plants. Totally 6750 plants were identified as point sources, including 191 power plants, 185 iron & steel plants, 231 cement factories, 707 lime and brick factories, 365 chemical plants and 5071 other industrial factories, as illustrated in Figure S2 in the supplement. In particular, the kilns for combustion and factories for calcination were separately investigated for cement production, and 25% of cement plants contained the both processes. For power, cement, and iron & steel sectors, the aggregated activity levels compiled plant by plant, i.e., the coal consumption of power generation, and the production of cement, clinker, coke, pig iron, and crude steel, were estimated at 108%, 95%, 120%, 109%, 104%, and 98% of the provincial statistics, respectively (JSNBS, 2013). The comparison indicates, on one hand, that larger activity levels would be obtained based on detailed investigation of individual emission sources than official statistics for power and most processes of iron & steel sectors. On the other hand, almost complete investigation on point sources was conducted for those sectors, as very small fractions of activities (5% for cement and 2% for steel production) had to be estimated as area sources. For other industrial sectors, smaller fractions of point sources were achieved, e.g., 32% and 36% for ammonia and

sulfuric acid production, respectively.

For on-road transportation, the input parameters of COPERT 4 include regional meteorological information, vehicle population by type, fleet composition by control stage (China I–IV, equivalent to Euro I–IV), average vehicle speeds, and annual average kilometers traveled (VKT). Monthly mean temperature and relative humidity were obtained from the China Meteorological Data Sharing Service System (http://www.escience.gov.cn). Populations of different vehicle types were derived from statistical yearbooks by city and then converted to the numbers in COPERT 4 categories. The fleet composition by control stage was obtained from the survey by local government (internal data, Zhao et al., 2015). Vehicle speed by road type (i.e., freeway, arterial and residential road) and VKT by vehicle type were determined according to previous studies (Cai and Xie, 2007; Wang et al., 2008) and the guidebook of emission inventory development for Chinese cities (He, 2015). For area sources, the coal consumption of residential activities was directly taken from National Energy Statistic Yearbook (NBSC, 2013c), while that of small industrial plants were calculated by subtracting the coal consumed by industrial point sources from the coal consumption of total industry provided in the provincial energy balance (NBSC, 2013c). The original data on the activity levels of agriculture, solvent use, non-road transportation and open biomass burning were obtained from the provincial or city statistical yearbooks (JSBNS, 2013).

2.3 Emission factor

Following previous studies (Zhao et al., 2008; 2010; 2011; 2012a; 2012b; Y. Zhao et al., 2013), an emission factor database for Jiangsu was established with detailed information and available results of emission measurements on local sources incorporated. For power sector, parameters relevant to emission factors were obtained at individual plant level including installed capacity, fuel type and quality (e.g., sulfur and ash content), combustion technology, and the type and removal efficiencies of APCDs. In particular, the information of APCD installation obtained from provincial environmental statistics and on-site survey was further corrected according to the official documents on APCD projects of power plants published by Ministry of Environment Protection of China (http://www.zhb.gov.cn/gkml/hbb/bgg/201305/t20130506_251654.htm). As summarized in

Table S2 in the supplement, the application rates of flue gas desulfurization (FGD), selective catalytic reduction (SCR)/selective non-catalytic reduction (SNCR), and dust collectors for Jiangsu's power plants in 2012 were 97%, 57% and 99% in terms of coal consumption, and the average removal efficiencies of SO_2, NOx and TSP weighted by coal consumption were calculated at 83.3%, 37.1% and 98.0%, respectively. Combining all the above-mentioned information, the emission factors for individual plant and facility were calculated using the methods developed by Zhao et al. (2010).

Table S3 in the supplement summarizes the emission factors of main industrial processes. For iron & steel production, emission factors of the four main manufacturing processes (coking, sintering, pig iron production, and steel making) were estimated combining the unabated emission factors from previous database (Zhao et al., 2011; Y. Zhao et al., 2013) and the investigated information on penetrations and removal efficiencies of APCDs at plant level. Provided in Table S2, 64.3% of Jiangsu's iron & steel plants installed FGD in 2012 and the average SO_2 removal efficiency was estimated at 78.0%. Dust collectors were installed at almost all the furnaces for pig iron production and steel making, with the averages of PM removal efficiency estimated at 96% and 94%, respectively. For cement production, emission factors were calculated for the two main processes, coal combustion and calcination, following Lei et al. (2011). With dust collectors installed at 99% of plants, the average of overall removal efficiency on TSP was estimated at 97.3% according to our plant-by-plant investigation (Table S2).

For area sources, emission factors for non-road transportation were obtained from Zhang et al. (2010), Ye et al. (2014) and Fu et al. (2012). Emission factors for household fossil fuel and biofuel combustion were from the summary of field measurements in Y. Zhao et al. (2013). For agricultural activities including livestock and fertilizer use, emission factors were obtained from Dong et al. (2009) and Yin et al. (2010). Emission factors of VOCs were mainly from Wei et al. (2009) with update for typical sources based on limited local measurements and survey (Bo et al., 2008; EEA, 2013; Xia et al., 2014). The source profiles of VOC for Jiangsu were obtained following Li et al. (2014) with the most recent data from domestic results incorporated (Zhao et al., in preparation).

2.4 Temporal and spatial distributions

The monthly variations of emissions from power plants and industrial sources were assumed to be dominated by the variations of electricity generation and typical industrial production, respectively, and those data were obtained from National Bureau of Statistics of China (http://data.stats.gov.cn/). As the real-time monitoring on urban traffic was unavailable for the whole province, the temporal distribution of emissions from on-road vehicles in other cities was considered to the same as Nanjing (Zhao et al., 2015). For other sources, the temporal distributions for Shanghai investigated by Li et al. (2011) were adopted.

Different parameters were used to conduct the spatial allocation of emissions by sector. Latitude and longitude of each point source collected from PSC were checked and revised according to Google Earth to avoid the unexpected errors in the existing database (Figure S2 in the supplement). The products of GDP (Huang et al., 2014) and population distribution with high resolution at 1km (Fu et al., 2014) were applied to allocate the emissions from industrial area sources and residential & commercial sources, respectively. Emissions from on-road transportation were allocated based on the road net by city. As the ship flow was unavailable, the widths of Yangtze River and the Grand Cannel within Jiangsu were used as indicators for ship emissions. Emissions from open biomass burning were allocated by the locations and brightness of agricultural fire spots observed by MODIS (Moderate Resolution Imaging Spectroradiometer, https://earthdata.nasa.gov/data/near-real-time-data/firms). NH_3 emissions from livestock and fertilizer usage were allocated based on the density of rural population and the distribution of agricultural lands obtained from the land utilization dataset GlobCover 2009 (http://globalchange.nsdc.cn).

2.5 Configuration of air quality modeling

The Models-3/Community Multi-scale Air Quality (CMAQ) version 4.7.1 was applied to evaluate the emission inventory for Jiangsu. As shown in Figure 1, three one-way nested domain modeling was conducted, and the spatial resolutions were set at 27, 9 and 3 km respectively in Lambert Conformal Conic projection, centered at (110° E, 34° N) with two true latitudes 25°N and 40°N. The mother domain (D1, 180×130 cells) covered most part of China, Japan and the whole Korea and part of other country. Jiangsu, Zhejiang, Shanghai,

Anhui and parts of other provinces were at the second modeling region (D2, 118×97 cells). The third (D3, 124×70 cells) covered the mega city Shanghai and six most developed cities in southern Jiangsu including Nanjing, Changzhou, Zhenjiang, Wuxi, Suzhou and Nantong. The simulation period was selected from October 1 to 31, 2012, with the first five days chosen as spin-up period to provide initial conditions for later simulations.

Meteorological fields were provided by the Weather Research and Forecasting Model (WRF) version 3.4 with the main physical options set as Fu et al. (2013), and the outputs were transferred by meteorology chemistry interface professor (MCIP) version 4.2 into the chemistry transport module in CMAQ (CCTM). In WRF, the U.S. Geological Survey (USGS) database was adapted as terrain and land use data, and the first guess field of meteorological modeling was provided by the final analysis dataset (ds083.2) from National Centers for Environmental Prediction (NCEP). Statistical indicators including Bias, Index of Agreement (IOA), and root mean squared error (RMSE) were applied to evaluate the performance of WRF modeling against observation (Baker, 2004; Zhang et al., 2006). Ground observations in three hours interval at meteorological stations were downloaded from National Climatic Data Center (NCDC), including 43 stations in the second modeling domain D2 and 7 stations in the innermost domain D3 (as labeled in Figure 1). The statistics of those indicators for wind speed and direction at 10 m (WS10 and WD10), temperature at 2 m (T2) and relative humidity at 2 m (RH2) for October 2012 in D2 and D3 were summarized in Table S4. Discrepancies between WRF simulations and ground observations were within acceptable range (Emory et al., 2001) and comparable to the results of other studies (Wang et al., 2014). Better agreements were found for simulations of T2 and RH2 than WS10 and WD10. In spite of moderate overestimation by 0.3% and 3.5% in T2 and RH2, the IOA of those two variables were 0.97 and 0.90, indicating the high consistency with observational. Slightly higher than observation in D2 and D3, simulated WS10 might enhance the diffusion process of pollutants in atmosphere eventually and thus lead to underestimation in pollutant concentrations. For WD10, the bias between simulations and observations was 3.6 degree in D3 within the benchmark range (Emory et al., 2001).

The carbon bond gas-phase mechanism (CB05) and AERO5 aerosol module were adopted in all the CMAQ modules. The initial concentrations and boundary conditions for

first modeling domain was the default clean profile, while for nested domain they were extracted from the CCTM outputs of its mother domain. Anthropogenic emissions used for domains D1 and D2 were obtained from the downscaled MEIC with an original spatial resolution of 0.25°×0.25°. For Jiangsu domain in D3, three inventories, i.e., downscaled MEIC, the regional inventory of YRD by Fu et al. (2013), and the provincial inventory developed in this work, were used to test the modeling performance and potential improvement in emission estimation. In addition, biogenic emission inventory was from the Model Emissions of Gases and Aerosols from Nature developed under the Monitoring Atmospheric Composition and Climate project (MEGAN-MACC, Sindelarova et al., 2014), and the emission inventories of Cl, HCl and lightning NO_X were from the Global Emissions Initiative (GEIA, Price et al., 1997). The vertical distributions of emissions were directly taken from L. Wang et al. (2010) except for the power sector, as the height of discharge outlet for each plant was available. According to L. Wang et al. (2010), the fractions of emissions of industry sources were 50%, 30% and 20% in layers 1-3, respectively. For the sources near the surface, i.e., transportation, residential & commercial combustion, solvent use, agriculture, and other, emissions were overall allocated to the first vertical layer in the model. The emissions of power plants were concentrated in layers 2-5 with the fractions estimated at 14%, 46%, 35% and 5%, respectively, based on the height information of the stacks.

3 RESULTS

3.1 Emission estimation and sector contribution

The total annual emissions of SO_2, NOx, CO, TSP, PM_{10}, $PM_{2.5}$, BC, OC, CO_2, NH_3 and VOCs were calculated at 1142, 1642, 7680, 2606, 1394, 941, 57, 138, 860458, 1100 and 1747 Gg for Jiangsu in 2012, respectively. The emissions by city were provided in Table 1. In general, higher emissions were found in cities in southern Jiangsu with large population and intensive economy and industry than those in northern Jiangsu. Taking 52% of the provincial industrial GDP, Suzhou, Nanjing, and Wuxi were estimated to collectively account for 41%, 41%, 35%, 31%, 43% and 39% of the total emissions of SO_2, NOx, CO, $PM_{2.5}$, CO_2 and VOCs, respectively. Xuzhou, different with other cities in northern Jiangsu, had a relative

high emissions of pollutants due to its well development of large-scale industry. Because of the active agricultural development, NH_3 emissions in Huai'an and Nantong were estimated at 195.9 and 187.1 Gg, significantly higher than other cities.

Shown in Figure 2 is the detailed sector contribution of pollutants from point, mobile (on-road transportation) and area sources. The point sources including power and industrial plants contributed 84%, 71%, 55%, 83%, 75%, 64%, 41%, 31%, 83%, 2% and 36%, to the total emissions of SO_2, NOx, CO, TSP, PM_{10}, $PM_{2.5}$, BC, OC, CO_2, NH_3 and VOCs, respectively. Notably the emission fractions of point sources were larger than those in other regional inventories (Fu, 2009; Tang et al., 2012; B. Zhao et al., 2012), resulting mainly from the compiling and application of information on individual power and industrial plants from varied data sources. Defined as area source, open biomass burning contributed 12%, 19%, 23%, 11% and 41% to the total CO, PM_{10}, $PM_{2.5}$, BC and OC, respectively.

The dominant contributors to SO_2 were power plant, iron & steel and other industry, with the emission fractions estimated at 38%, 10% and 45%, respectively. Although the coal consumption in power sector was 3.5 times larger than that in other industry sector (cement and iron & steel production excluded, JSNBS, 2013), smaller contribution to SO_2 emissions were found for coal-fired power plants, implying the benefits of strict control on SO_2 emissions from power sector. As shown in Table S2, the application rate and average SO_2 removal efficiency of FGD in power sector were significantly higher than those in other industry, suggesting the improvement in SO_2 abatement for industrial coal combustion other than power plants would be an effective measure to further reduce the emissions at present.

Power sector was the largest source for NO_X, contributing 41% to the total emissions, while the share of coal consumption of the sector reached 65% (JSNBS, 2013). It thus implied the tightened controls from implementation of new emission standard (GB13223-2011) and improved use of SCR/SNCR on power plants since 2011 compared to other sectors. Compiled from unit level, the average NOx removal efficiency of SCR/SNCR was calculated at 37% for Jiangsu's power plants in 2012 (Table S2), while Tian et al. (2013) estimated the values for SCR and SNCR at 70% and 25%, respectively, indicating the differences in assessment of emission controls for power sector between the provincial and national emission inventories with varied data sources. Transportation (including on-road and non-road) was estimated to be

the second largest sector for NO_X emissions, with the share to the total emissions calculated at 24%. Without specific control measures, cement and other industry were estimated to account for 7% and 18% of total NOx emissions.

CO was mainly generated from the manufacturing processes in iron & steel plants. The production of pig iron and crude steel in Jiangsu accounted for 9% and 10% to the national total in 2012, respectively (NBS, 2013), and was higher than other provinces in China except Hebei. Due to the intensive iron & steel industry, the contribution of the sector to the provincial total CO emissions was estimated at 35%. Residential biofuel combustion, open biomass burning and on-road transportation were also large contributors to CO with the emission fractions calculated as 24%, 12% and 11% respectively.

For particles, iron & steel and cement production were estimated to be the largest sources, contributing 24% and 27% to the total emissions of PM_{10}, and 27% and 19% to $PM_{2.5}$, respectively. Even with the largest coal consumption among all the sectors, the emissions from power plants were relatively small (6% and 4% to the total PM_{10} and $PM_{2.5}$ emissions, respectively), resulting mainly from the relatively high penetrations and removal efficiencies of dust collectors. Great differences existed in the sector distribution of BC and OC emissions. Iron & steel was estimated to be the largest source of BC, while open biomass burning and biofuel burning in residential stoves dominated OC, with the shares estimated at 41% and 29%, respectively. Moreover, as BC exhausted from the diesel engines was demonstrated to be higher than OC in previous situ measurements (He et al., 2015), BC emissions from non-road transportation (agricultural machines, rural vehicles, ships and construction machines) was estimated more than twice larger than OC.

For VOCs, solvent use and other industry including oil refinery, chemical industry and combustion were identified as the largest sources contributing 30% and 29% to total emissions, respectively. In particular, oil refinery and chemical engineering collectively accounted for 74% of the emissions of other industry. Due to lack of investigation on chemical industry plants, the fraction of area sources to the emissions of other industry reached 35%. Transportation and residential cooking are estimated to contribute 12% and 4% to total VOCs emissions, respectively. Livestock and fertilizer use were the two dominating sources of NH_3, with the shares to total emissions estimated at 47% and 45%, respectively.

For industry, ammonia production was the main source accounting for half of NH_3 emissions.

The spatial distribution of SO_2, NOx, CO, $PM_{2.5}$, VOCs and NH_3 emissions were at a resolution of 3×3km were illustrated in Figure S3 in the supplement. Outstandingly high emissions of SO_2, NOx, $PM_{2.5}$ and VOC indicated the existence of large industrial plants, particularly in Suzhou, Nanjing and Wuxi along with the Yangtze River. For CO and NOx, large emissions were distributed along the road net in the province, reflecting the important contribution of on-road transportation. Unlike other pollutants, high NH_3 emissions were more evenly distributed in rural areas as dominated by agricultural activities.

3.2 Comparisons with other studies

Figure 3 compares the emission estimations for Jiangsu between our provincial inventory and previous studies including two regional inventories (Fu et al., 2013; Li et al., 2011) and two national ones (MEIC; Xia et al., 2016). Note this work and Xia et al. (2016) reported the numbers for 2012, while Fu et al. (2013), Li et al. (2011) and MEIC were for 2010. As the emissions from open biomass burning were not included in other inventories except Fu et al. (2013) and this work, two values labeled as A and B were provided for our provincial inventory indicating the emissions with and without biomass open burning, respectively. While provincial economy and energy data were generally applied in all the national/regional inventories, information of individual large emitters were incorporated as well in MEIC, Fu et al. (2013) and Li et al. (2011). For example, the emissions of big plants for power generation, iron & steel and cement production in Jiangsu were partially investigated in Fu et al. (2013) and Li et al. (2011). For MEIC, large fraction of emissions from power generation sector was calculated plant by plant with relatively good data availability, while emissions from other industrial sectors were basically calculated at regional average and spatially allocated as area sources. The results in Fu et al. (2013) were generally smaller than those in other two inventories for 2010.

Attributed mainly to the improved use of FGD, the total SO_2 emissions were estimated to decline from 2010 to 2012 for the whole country (Xia et al., 2016) and typical city in Jiangsu (Zhao et al., 2015). It was reasonable to some extent that the SO_2 emissions in Jiangsu estimated in this work for 2012 was less than the 2010 results of Li et al. (2011) and MEIC.

Our estimation was 15% lower than the result for Jiangsu extracted from the national inventory by Xia et al. (2016), due mainly to the discrepancies in the penetration and SO_2 removal efficiency of FGD applied in the two inventories. Such information was obtained at provincial or national average level by Xia et al. (2016), in contrast to the provincial inventory based on investigation at plant level. For example, Xia et al. (2016) assumed that the penetration rates of wet and dry FGD technologies in coal-fired power sector were 83% and 5% in 2012, with the removal efficiencies estimated at 80% and 40%, respectively, and that there was not any SO_2 control in the remaining 11% of installed capacity at all. According to our plant-based investigation, the controls in Jiangsu were clearly enhanced, as shown in Table S2. As a result, SO_2 emissions from power sector was calculated at 430.0 Gg for Jiangsu 2012 in this work, 42% lower than those in Xia et al. (2016). The result for 2012 in our provincial inventory, however, is very close to the estimation by MEIC for 2010 (437.4 Gg), even though the coal consumption of power generation increased 29% for the period 2010-2012 (JSNBS, 2013). Besides the uncertainty in emission estimation from varied data sources of the two inventories, the improved use of FGD in the sector could be an important reason for the restrained emissions. Similar fact was found for Nanjing, the capital city of Jiangsu, that the SO_2 emissions of power generation calculated at city level kept stable along with a 25% growth of coal consumption from 2010 to 2012 (Zhao et al., 2015).

NOx emissions in our provincial inventory was slightly higher than those of Li et al. (2011) and clearly lower than the two national inventories. The major difference between the provincial inventory and MEIC was from industry, attributed probably to the application of varied emission factors. With different methods and data sources for certain sectors, the NOx emissions from industry were calculated at 388.1 and 566.2 Gg respectively by this work and Xia et al. (2016). For on-road transportation, the emission factors were estimated using CORPERT in this work, while they were obtained from limited domestic measurements in Xia et al. (2016). That was also the most important reason for the discrepancies in CO emission estimation between the two studies. For 2010, the NO_X emissions estimated by Fu et al. (2013) was 18% and 36% lower than those by Li et al. (2011) and MEIC, resulting mainly from the higher application rate and removal efficiency of SCR/SNCR technologies for power sector used in Fu et al. (2013).

The $PM_{2.5}$ and PM_{10} emissions in the provincial inventory were estimated to be 6% and 23% higher than those of Xia et al. (2016), and the sector contributions were notably different in the two inventories. For example, industry was estimated to contribute 77% and 80% of $PM_{2.5}$ and PM_{10} in the provincial inventory, much larger than the fractions at 45% and 52% by Xia et al. (2016), respectively. In this work, the $PM_{2.5}$ and PM_{10} emissions from cement production were calculated at 181 and 384 Gg, i.e., 2.5 and 2.0 times to those in Xia et al. (2016), and the analogue numbers for iron & steel production were 134 and 263 Gg, and 1.8 and 1.7 times, respectively. The discrepancies resulted mainly from the inconsistent penetration rates and removal efficiencies of dust collectors determined at national level and from on-site survey at provincial level. Taking cement as an example, all the plants were assumed to be installed with dust collectors, and the national average removal efficiency at 99.3% was applied in Xia et al. (2016), clearly larger than that from plant-by-plant survey as shown in Table S2. Note that the particle emissions in the provincial inventory were estimated higher than those in national ones including MEIC and Xia et al. (2016), while the gaseous pollutant emissions were lower except for NH_3 and CO_2. Compared to the emissions for 2010 estimated by other studies, the $PM_{2.5}$ and PM_{10} in our provincial inventory were 58% and 56% larger than Fu et al. (2013) (biomass open burning included), and 24% and 25% larger than Li et al. (2011) (biomass open burning excluded), respectively, beyond the growth rate of 20% for coal consumption during 2010-2012 (NBS, 2011; 2013).

The NH_3 emissions of Fu et al. (2013) and Li et al. (2011) were close to each other, while MEIC was only half of them for 2010. Using the results for 2006 from Huang et al. (2012), MEIC made a very low estimation in NH_3 emissions from livestock. The NH_3 emissions for 2012 in this work was calculated 11% and 22% larger than the results for 2010 by Fu et al. (2013) and Li et al. (2011), respectively. According to the provincial statistics, the total numbers of livestock and poultry increased 6% and 10% from 2010 to 2012 in Jiangsu (JSNBS, 2013). The growth of activity levels was expected to result in enhanced emissions, as very little progress was achieved for NH_3 control for these years.

3.3 Analysis of spatial distribution of emissions from given sectors

To further explore the discrepancies in emission estimation and spatial distribution from

varied data and emission allocation methods, comparisons between MEIC and our provincial inventory were conducted for pollutants from typical sources, including SO_2 from power plants, NO_X from transportation, and $PM_{2.5}$ from industry. The estimates in this work were reallocated into the 0.25°×0.25° grids, consistent with the spatial resolution of MEIC, and the correlation coefficients for emissions in all the grids can be calculated, as shown in Figure 4. Due mainly to the relatively transparent and easily available information of power plants, good consistency was found for SO_2 emissions from power sector in the two inventories, with the correlation coefficient calculated at 0.7 (Figure 4a). Even though the fundamental information of power plants in China is more accessible than other industry sources, mismatches still exist in different data sources. For example, some emission hotspots in our provincial inventory were not totally identical with those in MEIC in Suzhou, Nantong and Nanjing. In contrast to plant-by-plant investigation, the data from existing statistics at national level could not fully track the actual changes in the emitters, e.g., operation of new-built units, shutting down the small ones, or relocation of individual plants. In MEIC, moreover, the SO_2 emissions in several grids were estimated extremely small (less than 1 Mg), indicating that part of emissions from power sector was still allocated as area sources based on density of GDP or population. In contrast, all the plants were identified as point sources in the provincial inventory, based on the thorough investigation on individual sources.

For NO_X from transportation, the correlation coefficient was calculated at 0.8, indicating an even better consistency than SO_2 from power plants between the two inventories (Figure 4b). Although the difference in total emissions was small between our provincial inventory (682 Gg) and MEIC (722 Gg), the estimation of MEIC was notably higher than our result for northern Jiangsu including Yancheng, Huai'an and Suqian, implying the impacts from different ways for emission allocation. In this work, emissions from on-road vehicles were calculated and allocated based on road net that incorporates the information of transportation flow by road grade for each city. For non-road sources, large fraction of emissions was allocated based on the GDP density incorporated with land-use type. In national emission inventories, however, the emissions were first calculated at provincial level, and then downscaled at certain horizontal resolution. Despite of the discrepancies, it could be indicated by the relatively high spatial correlation between the two inventories that using GDP as proxy

for emission allocation would be acceptable when detailed information on road net and transportation flow was unavailable, since vehicles were largely concentrated in downtown with the intensive economic activity.

For $PM_{2.5}$ from industry, the correlation coefficient was calculated at 0.335, significantly lower than those mentioned above, indicating larger discrepancy in spatial distribution of industrial emissions between provincial and national inventories compared to power and transportation sectors. As shown in Figure 4c, the emission hotspots in the provincial inventory are highly consistent with the locations of large industrial $PM_{2.5}$ emitters (more than 10 Gg) estimated in this work, while the emission in MEIC were more distributed in developed cities (e.g., Suzhou) with high density of population or economy. Along with fast urbanization, super industrial sources have gradually been relocated to the rural and suburban areas, and the spatial correlation between industrial emissions and population could thus be weakened. In our provincial inventory, most industrial enterprises were identified as point sources, with the key parameters including geographic location, activity level and removal efficiency of dust collector investigated and corrected at plant level. In MEIC, the emissions were calculated using parameters at regional average level and allocated as area sources according to densities of population and/or economic activity. Without detailed information for individual sources, it might lead to errors in emission estimation and spatial distribution at regional or local scale. According to the survey at plant level, for example, only 20% of the lime factories were installed dust collectors in Jiangsu 2012, much lower than the value (roughly 90%) assumed in national inventories. As a result, the $PM_{2.5}$ emissions from industry were calculated at 570 Gg in our provincial inventory, 78% higher than those of MEIC.

4 ASSESSMENT OF THE PROVINCIAL EMISSION INVENTORY

4.1 Evaluation of spatial distribution of NO_X emissions with satellite observation

Tropospheric NO_2 vertical column density (VCD) retrieved from Ozone Monitoring Instrument (OMI) by the Royal Netherlands Meteorological Institute (Boersma et al., 2011) was employed to test the spatial distribution of NOx emissions in MEIC and this work. Tropospheric NO_2 over China in this product is consistent with NO_2 data from ground-based

measurements with multi-axis DOAS (R^2=0.96; Lin et al., 2014). Since clouds reduce the accuracy of satellite measurements, only pixels with cloud fraction$\leqslant$0.2 have been analyzed. NO_2 VCDs in summer were used due to the short lifetime of NO_2 in atmosphere at high temperature and the difficulty in accumulation for primary emissions with strong air convection. In addition, the summer prevailing wind for Jiangsu was generally from southeast where Shanghai and Zhejiang Province are located (see Figure S1 for the locations of the three regions). Total NO_X emissions of Jiangsu were estimated to be 65% and 282% larger than those of Zhejiang and Shanghai in MEIC, indicating the local sources played an important role in the air pollution formation for the province (Cheng et al., 2011). As Mijling et al. (2013) illustrated satellite observations could be used to evaluate the primary emissions for regions where NO_2 VCDs were mainly affected by local emissions, it was thus feasible to apply the OMI NO_2 VCDs in Jiangsu to assess its NOx emissions.

NO_2 VCDs in July 2010 and 2012 with original spatial resolution of 0.125°×0.125° were used for comparisons with the emissions in MEIC and our provincial inventory, respectively. To be consistent with MEIC, the emissions in our provincial inventory and the NO_2 VCDs from OMI were first upscaled to 0.25°×0.25° for the purpose of visualization and correlation analysis. As can be seen in Figure 5a and 5b, clear reduction in summer NO_2 VCDs was found in southern Jiangsu from 2010 to 2012, indicating the benefits of efforts on NO_X abatement since 2011. The NO_2 VCDs in the area along the Yangtze River were notably higher than that in other regions, attributed possibly to the substantial emissions from vessels and small captive power plants of the chemical and refinery industrial parks along the river without stringent controls as big power plants. Shown in Figure 5c and 5d are the spatial distributions of Jiangsu's NO_X emissions in MEIC and our provincial inventory, respectively， and the emission hotspots were generally consistent between the two inventories. Figure 5e and 5f shows the linear regression results between NO_2 VCDs and NOx emissions in MEIC and the provincial inventory, respectively. The correlation coefficients between VCDs and emissions were separately provided for all the grids and grids in different emission intervals, i.e., top 50%, 50%-75%, and last 25%.

The correlation coefficient between NO_2 VCDs and NOx emissions from the provincial inventory was 0.534, close to that between NO_2 VCDs and MEIC at 0.531. The result

indicated that there was no significant difference in spatial distribution of emissions between the national and provincial inventories at the relatively low horizontal resolution. However, great discrepancies existed when the correlation analysis was conducted for grids in different emission intervals. As shown in Figure 5e, the correlation coefficients between VCDs and MEIC emissions were calculated at 0.24 and 0.34, respectively, for the top 50% (20 grids with emissions ranged 32-121 Gg) and last 25% of gridded emissions (161 grids with emissions ranged 0-12 Gg). For our provincial emission inventory, the correlation coefficients were estimated slightly higher at 0.28 and 0.38, respectively, for the top 50% (18 grids with emissions ranged from 30-75 Gg) and last 25% of gridded emissions (176 grids with emissions ranged 0-12 Gg). Moreover, the coefficient between NO_2 VCDs and gridded emissions for the 50% -75% interval in provincial inventory was 0.26, while negative value (-0.07) was calculated for MEIC, indicating that the emission estimation for areas with small and medium sources in the provincial inventory was more consistent with satellite observation. To better quantify the emissions at local scale, the results revealed the practical significance of careful investigation on individual small industrial sources that were usually identified as area sources due to lack of detailed information in national or regional inventories.

The comparisons between spatial distribution of VCDs and emissions should be interpreted cautiously, particularly for regions with relatively low values, as the noise to signal ratio in OMI NO_2 increases with decreased VCDs. Moreover, although summer data were applied to mitigate the effects of long lifetime of NO_2 on pollution plums transport and chemical reaction, non-linear relationship still exists between emissions and VCDs. More comparisons between NO_2 from satellite observation and CTM are thus recommended when improved characterization of NO_2 vertical distribution is available for the region.

4.2 Evaluation of multi-scale inventories with CMAQ

As mentioned in Section 2.5, anthropogenic emission inventories at provincial, regional and national scales were applied respectively to explore the impacts of emission input on the performance of city-scale air quality simulation using CMAQ. With the original horizontal resolutions at 0.25×0.25 and 4×4 km, respectively, national (MEIC) and YRD regional inventories (Fu et al., 2013) were reallocated into the D3 of CCTM modeling at 3×3km

589 (Figure 1), consistent with our provincial inventory. The vertical and temporal distributions of
590 the two inventories were assumed to be same as those of our provincial inventory, as indicated
591 in Section 2.4. For the simulation with provincial inventory, emissions inside and outside
592 Jiangsu in D3 were taken from the provincial inventory developed in this study and from the
593 reallocated YRD regional inventory by Fu et al. (2013), respectively. Given the very limited
594 data accessible on air quality for the province in 2012, the available observation data at nine
595 state-operated monitoring sites in Nanjing including six urban sites (Xuanwumen (XWM),
596 Shanxilu (SXL), Zhonghuamen (ZHM), Ruijinlu (RJL), Caochangmen (CCM), and
597 Maigaoqiao (MGQ)), and three suburban sites (Pukou (PKS), Xianlin (XLS) and Olympic
598 sports center (OSC)) were applied to evaluate the simulation performances with different
599 emission inputs (see locations of the nine sites in Figure 1).

600 The hourly ground concentrations from observation and CMAQ simulation for October
601 2012, expressed as the averages for all the monitoring sites in Nanjing, were compared and
602 illustrated in Figure S4 in the supplement for SO_2, NO_2, ozone and $PM_{2.5}$. Even though all the
603 simulations could well reproduce the time variation of each species, discrepancies existed
604 when different anthropogenic emission inventory were used. The simulated SO_2 and NO_2
605 concentrations using the provincial inventory were notably lower than those with other two
606 inventories. In addition, simulations failed to catch the high $PM_{2.5}$ and O_3 concentrations for
607 some heavy polluted episodes. For example, the average $PM_{2.5}$ ground concentration during
608 October 21st-23rd and 28th-29th were simulated at 40 and 31 μg/m^3, 1.4 and 3.2 times lower
609 than observations. Two statistical indicators, normalized mean bias (NMB) and normalized
610 mean error (NME), were applied to evaluate the model performance (Zhang et al., 2006), as
611 summarized in Table 2. Among all the species, the best simulation performance was found for
612 NO_2, with the NMBs ranged within ±30% for different emission. In general, simulations
613 using the provincial emission inventory performed notably better than those with national and
614 regional ones for all the species, and the NMEs and NMBs were calculated at 47%, 33%,
615 44%%, 52% and -10%, -14%, -25%, -43% for SO_2, NO_2, O_3, $PM_{2.5}$ respectively, comparable
616 to previous U.S. studies (Zhang et al., 2006; Wang et al., 2009). The result thus partly
617 confirmed that air quality simulation at local or regional scales would be largely improved

618 when detailed information on individual sources could be incorporated in the emission
619 inventory. Improved model prediction for pollution event was also achieved with provincial
620 inventory. Taking the pollution episode between 8pm on 18th and 5pm on 19th October as an
621 example, the observed $PM_{2.5}$ concentration at CCM site kept increasing from 8pm on 18th with
622 the highest value reaching 114 μg/m^3 at 2am on 19th. Simulated $PM_{2.5}$ concentrations with
623 provincial, regional and national inventory at that time were 90, 53 and 45 μg/m^3, respectively.
624 The correlation coefficients between observation and simulations with the three inventories
625 were calculated as 0.66, 0.44 and 0.30 during the episode, respectively, indicating the
626 advantage of provincial inventory in the pollution event simulation.

627 Compared to primary pollutants SO_2 and NO_2, species with strong secondary formation
628 process ($PM_{2.5}$ and O_3 in this case) were clearly under predicted by CMAQ, no matter which
629 inventory was applied. Lack of dust emissions in inventories might be one reason for
630 underestimation of $PM_{2.5}$. Moreover, as the significant composition of $PM_{2.5}$ in eastern China
631 (Yang et al., 2011), secondary organic and inorganic aerosols might be under predicted
632 attribute to the weakness of chemical mechanisms in the version of CMAQ including the
633 transformation of sulfate and the formation of secondary organic aerosols (Wang et al., 2009).
634 For ozone simulation, better performance was found at suburban sites than urban sites, and
635 the lower simulated concentrations than observation could possibly come from the
636 underestimation in precursor VOCs emissions. For example, the NMB was estimated at -26%
637 for PKS, where many chemical industrial plants were located nearby. In addition, the
638 uncertainty of NO_X emission estimation might also contribute to the discrepancy. As indicated
639 by the data from available continuous emission monitoring systems on Jiangsu's power plants,
640 the NO_X emission factors of power sector applied in current inventory might be overestimated
641 for 2012 (unpublished).

642 The total emissions of SO_2 and NOx in Jiangsu estimated by Fu et al. (2013) was 1126
643 and 1257 Gg, i.e., 9% and 22% lower than the results of our provincial inventory, respectively.
644 Using the regional inventory by Fu et al. (2013), much higher concentrations of SO_2 and NO_2
645 were simulated than observation at the monitoring sites, with the NMBs calculated at 74%
646 and 30%, respectively. Even with larger emissions, in contrast, the NMBs for simulation with

our provincial inventory were -10% and -14%, indicating lower simulated concentrations than observation. This result implies the possible impacts of spatial distributions of emissions on air quality modeling. In regional inventory, densities of population and economic activities were generally applied to allocate large fraction of emissions, leading to particularly high emissions in urban areas, as the economy and population was generally centralized in downtown. Given all the monitoring sites in Nanjing are located in urban or suburban areas, air quality simulation using regional emission inventory was thus liable to over predict the ground concentrations at those sites.

Spatial distributions of the monthly mean for simulated concentrations using national, regional and provincial inventories were plotted for SO_2, NO_2, $PM_{2.5}$ and O_3 in Figure 6, and the differences between simulations with varied emissions were shown in Figure 7. As the MEIC emissions were greatly averaged when they were directly downscaled from 0.25°×0.25° to 3×3 km, the simulated high concentrations using MEIC were broadly distributed in the modeling domain and commonly located in downtown (as indicated in Figure S1), with the large emitters hardly identified (Figure 6a). For results using the regional and provincial inventories, there were several grids with notably outstanding simulated concentrations, indicating the existence of large emitters (Figure 6b and 6c), and differences with the simulation using MEIC were induced (Figure 7a and 7b). As shown in Figure 7c, moreover, clear differences were also detected between simulations using regional and provincial inventories, implying the discrepancy in allocations of high emissions between the two inventories. With the locations of large power, iron & steel, and cement plants incorporated, the YRD regional emission inventory by Fu et al. (2013) allocated a large fraction of emissions from industries as area sources. In contrast, the emissions from most power and industrial plants were calculated based on source-specific information and were precisely allocated in the provincial inventory, avoiding particularly the emission overestimation in downtown. In addition, the simulated NO_2 and O_3 concentrations for regions outside Jiangsu (i.e., Shanghai and part of Zhejiang and Anhui) using the provincial inventory were 22% lower and 40% higher in average than those using the regional one, respectively (Figure 7c), although same emissions (Fu et al., 2013) were used outside Jiangsu for the two inventories. The result indicates that both local and regional emissions were

important for the simulations of the secondary pollutant like O_3. Total VOCs emissions for Jiangsu were estimated at 1740 Gg in MEIC, slight higher than those in the regional (1659 Gg) and provincial inventory (1617 Gg), while the simulated monthly mean O_3 concentrations within Jiangsu using MEIC were notably lower than those using the latter two emissions. Categorized by CB05, differences in chemical compositions of VOCs could be found in the three inventories, attributed to the varied source contributions to VOC emissions and to the different source profiles used in emission speciation (Zhao et al., in preparation). For example, the emissions of ethane (ETH) and ethanol (ETHA) with relatively high ozone formation potential in the provincial inventory were 44% and 209% higher than those in MEIC, respectively. Therefore, the total emission amount, spatial distribution of emissions, and the chemical compositions of precursors are all crucial to the accuracy of ozone simulations, and further analysis on those factors are suggested.

4.3 Improved SO_2 simulation under special meteorological condition

To further examine the simulated concentration response to varied emission inputs at local scale, the simulated SO_2 concentrations using national, regional and provincial inventories were compared with observation at three monitoring sites in downtown Nanjing (XWH, RJL and ZHM) for 6^{th} -14^{th} October 2012, as illustrated in Figure 8. The simulated concentrations using our provincial inventory were the most consistent with observation, while apparent overestimation was found for the simulations using national or regional inventories. At 8 pm October 9 (local time), in particular, the SO_2 concentrations were observed at 33, 12, and 14 $\mu g/m^3$ at XWH, RJL and ZHM sites, respectively, while the simulated concentrations were respectively simulated at 205, 246 and 228 $\mu g/m^3$ using MEIC, i.e., 5-19 times higher than the observation. The analogue numbers with regional inventory by Fu et al. (2013) even reached 550, 477 and 476$\mu g/m^3$, i.e., 15-38 times higher than observation. Although concentrations remained over predicted, better performance was achieved when the improved provincial inventory was used, implying its advantage prior to national or regional ones in the high-resolution air quality modeling. The discrepancies in emissions and the simulated meteorological condition including wind velocity and height of planetary boundary layer (PBL) were inspected to understand the very high concentrations

706 from simulation.

707 Figure S5 in the supplement shows the simulated wind fileds from 2 pm on 9th to 5am on
708 10th October. From 2 pm on 9th October 9, WS10 in downtown Nanjing started to decline
709 gradually and reached the minimum of 0.22 m/s at 8 pm, simply not beneficial for the
710 horizontal convection of atmosphere. In addition, the monthly average of PBL height at XWH
711 was simulated at 485 m at day and 140 m at night in October. From 5pm on 9th to 10am on
712 10th, however, the average PBL height decreased to 39m, with the minimum simulated at 32
713 m at 11pm on 9th, seriously restricting the vertical diffusion of pollutants. Under the
714 meteorological condition that horizontal and vertical movement of atmosphere were limited,
715 primary pollutants from large emitters would be easily accumulated over time, possibly
716 leading to high concentrations for areas close to the emission sources. In this case, therefore,
717 the simulated SO_2 concentrations would be largely influenced by the emissions from local and
718 nearby sources, as discussed below.

719 The total SO_2 emissions in Nanjing were estimated at 141 Gg in the provincial inventory,
720 2% and 7% higher than those of national and regional ones respectively. Without big
721 difference in total amount, large discrepancies in spatial distribution existed in those
722 inventories, particularly at high horizontal resolution as shown in Figure 9. Downscaled from
723 0.25°×0.25° to 3×3 km, grids with similar emissions were clustered for MEIC and spatial
724 variations in emissions could hardly be detected other than the hotspot in downtown (Figure
725 9c). Notably lower emissions in downtown Nanjing were found in our provincial inventory
726 than the regional one (Figure 9a and 9b). In addition, the grid with maximum SO_2 emissions
727 (15.7 Gg) in the provincial inventory was in the northwestern of Nanjing where a super power
728 plant was located, labeled as the black star (point A) in Figure 9. As a comparison, the grid
729 with the maximum SO_2 emissions in the regional inventory labeled as the black triangle (point
730 B) in Figure 9 was adjacent to the location of A, and its emissions were calculated to be only
731 28% of the result in the provincial one. Given no other super emitters located nearby, we
732 expected that the discrepancy resulted mainly from the varied emission estimation and
733 positioning for the same power plant in the two inventories. According to on-site survey, only
734 one unit out of two for the plant was installed with FGD, and the SO_2 emissions of the plant
735 was estimated at 13.6 Gg, accounting for 87% of the total emissions in the grid. In contrast, a

736 higher FGD installation rate at 85% was uniformly assumed for the power sector in the
737 regional inventory by Fu et al. (2013), leading to possible underestimation in emissions for
738 the plant. The comparison implied that detailed information compiled from individual plants
739 were crucial for estimation and spatial distribution of pollutant emissions at local scales. SO_2
740 emissions at given monitoring sites were extracted from the gridded national, regional and
741 provincial inventories and summarized in Table 3. As most large SO_2 emitters were located in
742 suburban or rural areas, relatively small emissions were found in the provincial inventory for
743 downtown Nanjing where the monitoring sites were located. As large fractions of emissions
744 were allocated by the density of economy and population, however, the SO_2 emissions in the
745 regional emission inventory were estimated at 1791, 1721, 1918, and 1635 Mg at XWH, RJL,
746 ZHM and CCM sites, which were 4-5 times higher than those of our provincial inventory. In
747 MEIC, the emissions at XWH, RJL, ZHM and MGQ sites were identically estimated at 1298
748 Mg from the downscaling approach, and they were also much larger than those in the
749 provincial inventory. Given the unfavorable condition of pollutant transport for 9^{th}-10^{th}
750 October, the overestimation in local emissions around the downtown monitoring sites in the
751 national and regional inventories thus lead to terribly high simulated concentrations, while the
752 results using the provincial one were much more reasonable. The comparison confirms the
753 benefits of precise quantification of emissions on local air quality modeling.

754 Despite of significant improvement, overestimation in SO_2 concentrations still existed in
755 the simulation with our provincial inventory, attributed possibly to the error of meteorology
756 modeling. Here we selected XWH site as an example to conduct the back trajectory analysis
757 using HYSPLIT model (http://ready.arl.noaa.gov/HYSPLIT.php). Shown in Figure S6 in the
758 supplement, the air mass reaching the site at 50 m altitude came mainly from northeast at
759 11pm on 9^{th} October. However, it was inconsistent with WRF modeling results, which
760 indicated the dominating wind was from northwest (150°-170°) at that time. As mentioned
761 above, a big power plant was located northwest to XWH (Figure 9a), and the site might partly
762 be influenced by the large emissions from the plant and enhanced concentrations would then
763 be obtained when northwest wind was simulated.
764

5 SENSITIVITY ANALYSIS OF $PM_{2.5}$ AND OZONE FORMATION IN NANJING

Using the improved provincial inventory, the sensitivity of $PM_{2.5}$ and O_3 concentrations to emissions were further analyzed through the Brute-Force method (BFM, Dunker et al., 1996). For $PM_{2.5}$, four simulation scenarios were designed: Scenario B (the base case) in which the emissions from all types of sources are included; and Scenarios S1, S2, and S3 in which the pollutant emissions of power, iron & steel and cement plants in D3 were zero out, respectively. The changes in simulated $PM_{2.5}$ ground concentrations in S1, S2, and S3 compared to those in base case for October 2012 are illustrated in Figure S7 in the supplement. The average concentration increments in urban area of Nanjing caused by power, iron &steel, and cement plants were calculated respectively at 3, 11 and 7 $\mu g/m^3$, accounting for 6%, 26% and 16% of the monthly mean $PM_{2.5}$ concentrations, and the maximum increments within the domain reached 10, 72, and 25 $\mu g/m^3$, respectively. Given the tiny emission fraction of power sector for primary $PM_{2.5}$ (4% in Jiangsu Province) and the small share in the ground layers (15% for 1st plus 2nd vertical layers), its contribution to $PM_{2.5}$ ground concentration was notably lower than those of iron & steel and cement. Summarized in Table 4 are the contributions of power, iron & steel, cement sectors to monthly mean $PM_{2.5}$ at the nine monitoring sites in Nanjing, October 2012. The contributions of the three sectors to average $PM_{2.5}$ concentrations at all the sites were estimated at 8%, 13% and 9%, respectively. Since all the sites are located in the urban or suburban areas, the estimated $PM_{2.5}$ contributions at individual site varied slightly to each other. Besides monthly mean, the hourly maximum and minimum contributions are provided as well in Table 4. The largest hourly contributions from power, iron & steel and cement plants to $PM_{2.5}$ concentrations were 65% at PKS, 89% at MGQ and 58% at both CCM and OCS, respectively. The contributions became negative at 2 pm on 26th October with average $PM_{2.5}$ concentration of all the sites observed as 164 $\mu g/m^3$ and simulated as 151 $\mu g/m^3$ under the base case, i.e., increased particle concentrations were simulated at the moment when emissions from given sector was turned off. The result indicated, on one hand, the relatively high uncertainty of simulation for heavy PM pollution episode dominated by regional transport. On the other hand, as the simulated increments were mostly from the elevated sulfate (SO_4^{2-}), nitrate (NO_3^-) and ammonium (NH_4^+), the negative

794 contributions might also be caused by the complex chemical mechanisms of SO_2 and NOx
795 reactions with NH_3 under the NH_3-rich condition in YRD (Wang et al., 2011). Intensive
796 real-time observation on chemical composition of $PM_{2.5}$ is thus recommended to better
797 capture and analyze the processes.

798 To explore the sensitivity of O_3 formation to its precursor emissions, two scenarios were
799 set besides the base case: the VOC-abatement scenario with 50% reduction of all
800 anthropogenic VOCs emissions in D3 (Scenario P1), and the NOx-abatement scenario with
801 50% reduction of NOx in D3 (Scenario P2). Shown in Figure S8 in the supplement were the
802 average O_3 concentration changes from October 6th to October 15th. The simulated O_3 average
803 concentration from 11am to 5pm declined significantly under Scenario P1, with the maximum
804 reduction at 54 μg/m^3 (Figure S8a) within D3, and changes in the downwind region were
805 greater than the upwind. In contrast, the concentrations were generally enhanced under P2
806 with the maximum increment at 19 μg/m^3. Similar variation pattern was found for 1-hour
807 maximum O_3 concentration in Figure S8b and monthly mean concentration in Figure S8c.
808 The 1-hour maximum O_3 concentrations in most downwind area of Shanghai and southern
809 Jiangsu decreased 10-20 μg/m^3 with the reduction in VOCs emissions, and the concentrations
810 would generally increase 10-30 μg/m^3 with the NO_X reduction. The similar patterns of O_3
811 concentration variation in urban and downwind areas in D3 under P1 or P2 scenario indicated
812 that the O_3 formation was VOCs-limited in all those areas in southern Jiangsu. Therefore,
813 VOC emission abatement could be effective for O_3 pollution control in southern Jiangsu,
814 while NO_X abatement might aggravate the pollution in autumn.

815 The temporal changes in the simulated O_3 concentrations between the P1/P2 and base
816 scenarios at urban (XWH, SXL, RJL, MGQ, ZHM and CCM) and suburban sites (XLS, OCS
817 and PKS) in Nanjing were illustrated for October 6th-16th in Figure 10. Simulated O_3
818 concentrations at urban and suburban sites were generally decreased once the VOC emissions
819 declined and the maximum hourly reduction reached 77.3 and 49.6 μg/m^3, respectively. In
820 contrast, concentrations were elevated with the NOx emission reduction and the maximum
821 growth were 78.7 and 15.4 μg/m^3, respectively. Under VOCs-limited regime, in general, the
822 O_3 concentration would be little sensitive to the change of NOx unless it was rich enough to
823 turn to the negative correlation with O_3. Therefore, due to the intensive NOx emissions from

824 on-road transportation in downtown Nanjing, the variations of O_3 concentrations in P2
825 scenario at urban monitoring sites were notably greater than those at suburban sites. It should
826 be acknowledged that uncertainty existed in the sensitivity analysis, as the brute-force method
827 ignores the nonlinearity of O_3 response to the changes of precursor emissions. With
828 techniques other than brute-force, e.g., ozone source apportionment (OSAT, Li et al., 2012) or
829 tagged species method (Zhang et al., 2011), the nonlinearity mechanism of O_3 formation
830 could be taken into account. Comparisons between results with different methods are further
831 recommended for the region.
832

833 ## 6 CONCLUSIONS

834 The bottom-up approach was applied to develop a high-resolution emission inventory for
835 Jiangsu, with substantial detailed information on local sources incorporated. Key parameters
836 relevant to emission estimation were examined and revised plant by plant including
837 geographic position, energy consumption and removal efficiencies of APCD from various
838 data sources and on-site survey on large emitters. Compared to previous studies, the emission
839 fractions of point sources were significantly enhanced, except for NH_3 and OC, which are
840 mainly from agriculture activities and biomass open burning, respectively. As lower removal
841 efficiencies of dust collectors were obtained from local investigation, larger primary PM
842 emissions were estimated in our provincial inventory than other national or regional ones.
843 Moreover, clear discrepancy existed in spatial distribution of industrial $PM_{2.5}$ emissions
844 between this work and the national inventory MEIC, indicating the uncertainty of emission
845 downscaling from coarse horizontal resolution. The spatial distribution of NO_X emissions in
846 the provincial inventory was more consistent with summer tropospheric NO_2 VCDs observed
847 from OMI than that of MEIC, particularly for the emissions from small and medium industrial
848 plants. WRF-CMAQ air quality modeling system was set up to evaluate the reliability and
849 improvement of the provincial emission inventory by comparing the simulation performance
850 with that using a national (MEIC) and regional one. Among the three inventories, the best
851 agreement was found between the observation and simulation with the provincial one for all
852 the concerned species at the nine monitoring sites in Nanjing, while underestimation existed

853 particularly for $PM_{2.5}$ and O_3 that were strongly influenced by secondary formation. Under the
854 unfavorable meteorology of pollutant transport, extremely high SO_2 concentrations were
855 simulated using the regional and national inventories, while the results using provincial one
856 were much closer to the observation. The results indicated the advantage of improved
857 estimation and spatial distribution of emissions on air quality modeling at regional or local
858 scales. The improved provincial inventory was further applied for the sensitivity analysis on
859 $PM_{2.5}$ and O_3 formation using BFM simulation, and provided the preliminary results for the
860 policy making of regional haze and photochemical pollution control in southern Jiangsu.

861 Limitations remained in the current inventory. Attributed to unavailability of detailed
862 information, the weekly and hourly variation of emissions could not be fully tracked for each
863 city, and the vertical distribution of emissions by sector, depending mainly on the stack height,
864 temperature and flow of flue gas, could not be accurately determined. Instead, empirical data
865 from previous work (Li et al., 2011; L. Wang et al., 2010; 2014) had to be applied, which
866 might be inconsistent with the reality. In addition, some sources were not included in the
867 current inventory, e.g., fugitive dust emissions from construction sites and road transportation,
868 resulting from lack of reliable data and thereby potentially large uncertainties in the emission
869 estimation at provincial level. Finally, the effects of source profiles on air quality modeling,
870 e.g., the speciation of primary $PM_{2.5}$ and VOC, were not fully evaluated. As they are
871 important on the formation of O_3 and secondary particles, more investigations on typical
872 sources and evaluation through chemistry transport modeling are suggested in the future.
873

874 **ACKNOWLEDGEMENT**

875 This work was sponsored by the Natural Science Foundation of China (41575142),
876 Natural Science Foundation of Jiangsu (BK20140020), Jiangsu Science and Technology
877 Support Program (SBE2014070918), and Special Research Program of Environmental
878 Protection for Commonweal (201509004). We would like to acknowledge Litao Wang from
879 Hebei University of Engineering, Jia Xing from Tsinghua University for the assistance in
880 CMAQ model, and Xiao Fu from Tsinghua University for providing the emission inventory
881 for Yangtze River Delta region, China.

882

883 **REFERENCES**

884 Baker: Meteorological modeling protocol for application to $PM_{2.5}$/haze/ozone modeling
885 projects, 2004.

886 Bo, Y., Cai, H., Xie, S. D.: Spatial and temporal variation of historical anthropogenic
887 NMVOCs emission inventories in China, Atmos. Chem. Phys., 23, 7297-7316, 2008.

888 Boersma, K. F., Eskes, H. J., Dirksen, R. J., van der A, R. J., Veefkind, J. P., Stammes, P.,
889 Huijnen, V., Kleipool, Q. L., Sneep, M., Claas, J., Leitão, J., Richter, A., Zhou, Y., and
890 Brunner, D.: An improved tropospheric NO2 column retrieval algorithm for the Ozone
891 Monitoring Instrument, Atmos. Meas. Tech., 4, 1905–1928, doi:10.5194/amt-4-1905-2011,
892 2011.

893 Cai, H., Xie, S. D.: Estimation of vehicular emission inventories in China from 1980 to 2005,
894 Atmos. Environ., 41, 8963-8979, 2007.

895 Cheng, Z., Chen, C. H., Huang, C., Huang, H. Y., Li, L., Wang, H. L.: Trans-boundary.
896 primary air pollution between cities in the Yangtze River Delta. Acta Sci. Circum., 31,
897 686-694, 2011 (in Chinese).

898 Dong, Y. Q., Chen, C. H., Huang, C., Wang, H. L., Li, L., Dai, P., Jia, J. H.: Anthropogenic
899 emissions and distribution of ammonia in Yangtze River Delta, Acta Sci. Circum., 29,
900 1611-1617, 2009 (in Chinese).

901 Dunker, A. M., Morris, R. E., Pollack, A. K., Schleyer, C. H., and Yarwood, G.:
902 Photochemical modeling of the impact of fuels andvehicles on urban ozone using auto oil
903 program data, Environ. Sci. Technol., 30, 787–801, 1996.

904 EEA (European Environment Agency): COPERT 4-Computer Programme to Calculate
905 Emissions from Road Transport, User Manual (Version 9.0), Copenhagen, Denmark, 2012.

906 EEA (European Environment Agency): EMAP/CORINAIR Emission Inventory
907 Guidebook-2013, http://www.eea.euopa.eu//publications/emep-eea-guidebook-2013, 2013.

908 Emery, C., Tai, E., Yarwood, G.: Enhanced meteorological modeling and performance
909 evaluation for two Texas episodes, Report to the Texas Natural Resources Conservation
910 Commission, prepared by ENVIRON, International Corp, Novato, CA, 2001.

911 Fu, J. Y., Jiang, D., Huang, Y. H.: 1Km Grid Population Dataset of China
912 (PopulationGrid_China), Global Change Research Data Publishing & Repository,
913 DOI:10.3974/geodb.2014.01.06. V1, 2014.

914 Fu, M. L., Ge, Y. S., Tan, J. W., Zeng, T., Liang, B.: Characteristics of typical non-road
915 machinery emissions in China by using portable emission measurement system, Sci. Total
916 Environ., 437, 255-261, 2012.

917 Fu, Q. Y.: Emission inventory and the foundation mechanism of high pollution of fine
918 particulate matters in Shanghai (in Chinese), Ph. D thesis, Fudan University, Shanghai, China,

2009.

Fu, X., Wang, S. X., Zhao, B., Xing, J., Cheng, Z., Liu, H., and Hao, J. M.: Emission inventory of primary pollutants and chemical speciation in 2010 for the Yangtze River Delta region, China, Atmos. Environ., 70, 39-50, 2013.

Han, K. M., Lee, S., Chang, L. S., and Song, C. H.: A comparison study between CMAQ-simulated and OMI-retrieved NO_2 columns over East Asia for evaluation of NOx emission fluxes of INTEX-B, CAPSS, and REAS inventories, Atmos. Chem. Phys., 15, 1913-1938, doi:10.5194/acp-15-1913-2015, 2015.

He, K. B.: Multi-resolution Emission Inventory for China (MEIC): model framework and 1990–2010 anthropogenic emissions, International Global Atmospheric Chemistry Conference, 17–21 September, Beijing, China, 2012.

He, K. B. (eds): Guidebook of Air Pollutant Emission Inventory Development for Chinese Cities, Beijing, 2015 (in Chinese).

He, L. Q., Hu, J. N., Zu, L., Song, J. J., Chen, D.: Emission characteristics of exhaust $PM_{2.5}$ and its carbonaceous components from China I to China III heavy-duty diesel vehicles, Acta Scientiae Circumstantiae, 35, 656-662, 2015 (in Chinese).

Huang, C., Chen, C. H., Li, L., Cheng, Z., Wang, H. L., Huang, H. Y., Streets, D. G., Wang, Y. J., Zhang, G. F., and Chen, Y. R.: Emission inventory of anthropogenic air pollutants and VOC species in the Yangtze River Delta region, China, Atmos. Chem. Phys., 11, 4105-4120, 2011.

Huang, R. J., Zhang, Y., Bozzetti, C., Ho, K. F., Cao, J. J., Han, Y., Daellenbach, K. R., Slowik, J. G., Platt, S. M., Canonaco, F., Zotter, P., Wolf, R., Pieber, S. M., Bruns, E. A., Crippa, M., Ciarelli, G., Piazzalunga, A., Schwikowski, M., Abbaszade, G., Schnelle- Kreis, J., Zimmermann, R., An, Z., Szidat, S., Baltensperger, U., Haddad, I. E., and Prevot, A. S.: High secondary aerosol contribution to particulate pollution during haze events in China, Nature, 514, 218–222, 2014.

Huang, X., Song, Y., Li, M. M., Li, J. F., Huo, Q., Cai, X. H., Zhu, T., Hu, M., and Zhang, H. S.: A high-resolution ammonia emission inventory in China Global Biogeochem, Cycles, 26: GB1030, doi:10.1029/2011GB004161, 2012.

Huang, Y. H., Jiang, D., Fu, J. Y.: 1Km Grid GDP Data of China (2005, 2010) (GDPGrid_China), Global Change Research Data Publishing & Repository, DOI:10.3974/geodb.2014.01.07. V1, 2014.

Huo, H., Wang, M., Zhang, X. L., He, K. B. Gong, H. M., Jiang, K. J., Jin, Y. F., Shi, Y. D., Yu X.: Projection of energy use and greenhouse gas emissions by motor vehicles in China: Policy options and impacts, Energ. Policy, 43: 37-48, 2012.

JSNBS (Jiangsu Bureau of Statistics): Statistical Yearbook of Jiangsu, Beijing, China Statistics Press, 2011 (in Chinese).

JSNBS (Jiangsu Bureau of Statistics): Statistical Yearbook of Jiangsu, Beijing, China

957 Statistics Press, 2013 (in Chinese).

958 Kain, J.: The Kain-Fritsch convective parameterization: An update, J. Appl. Meteor., 43,
959 170-181, 2004.

960 Kurokawa, J., Ohara, T., Morikawa, T., Hanayama, S., Janssens-Maenhout, G., Fukui, T.,
961 Kawashima, K., and Akimoto, H.: Emissions of air pollutants and greenhouse gases over
962 Asian regions during 2000–2008: Regional Emission inventory in Asia (REAS) version 2,
963 Atmos. Chem. Phys., 13, 11019–11058, doi:10.5194/acp-13-11019-2013, 2013.

964 Lei, Y., Zhang, Q., Nielsen, C., He, K. B.: An inventory of primary air pollutants and CO_2
965 emissions from cement production in China, 1990-2020, Atmos. Environ., 45, 147-154, 2011.

966 Li, L., Chen, C. H., Fu, J. S., Huang, C., Streets, D. G., Huang, Y. H., Zhuang, G. F., Wang, J.
967 Y., Jang, C. J., Wang, H. L., Chen, Y. R., and Fu, M. J.: Air quality and emissions in the
968 Yangtze River Delta, China, Atmos. Chem. Phys., 11, 1621-1639,
969 doi:10.5194/acp-11-1621-2011, 2011.

970 Li, M., Zhang, Q., Streets, D. G., He, K. B., Cheng, Y. F., Emmons, L. K., Huo, H., Kang, S.
971 C., Lu, Z., Shao, M., Su, H., Yu, X., and Zhang, Y.: Mapping Asian anthropogenic emissions
972 of non-methane volatile organic compounds to multiple chemical mechanisms, Atmos. Chem.
973 Phys., 14, 5617-5638, 2014.

974 Lin, J., Martin, R. V., Boersma, K. F., Sneep, M., Stammes, P., Spurr, R., Wang, P., van
975 Roozendael, M., Clémer, K., and Irie, H.: Retrieving tropospheric nitrogen dioxide from the
976 Ozone Monitoring Instrument: effects of aerosols, surface reflectance anisotropy, and vertical
977 profile of nitrogen dioxide, Atmos. Chem. Phys., 14, 1441-1461, 2014

978 Ministry of Environmental Protection (MEP): China National Ambient Air Quality Standards,
979 GB3095-2012, MEP, Beijing, China, 2012 (in Chinese).

980 Mijling, B., Vander, A. R. J., Zhang, Q.: Regional nitrogen oxides emission trends in East
981 Asia observed from space, Atmos. Chem. Phys., 13: 12003-12012, 2013.

982 National Bureau of Statistics (NBS): China Statistical Yearbook 2013, China Statistics Press,
983 Beijing, 2013a (in Chinese).

984 National Bureau of Statistics (NBS): China Industry Economy Statistical Yearbook 2012,
985 China Statistics Press, Beijing, 2013b (in Chinese).

986 National Bureau of Statistics (NBS): China Energy Statistical Yearbook 2012, China Statistics
987 Press, Beijing, 2013c (in Chinese).

988 Ohara, T., Akimoto, H., Kurokawa, J., Horii, N., Yamaji, K., Yan, X., and Hayasaka, T.: An
989 Asian emission inventory of anthropogenic emission sources for the period 1980–2020,
990 Atmos. Chem. Phys., 7, 4419–4444, doi:10.5194/acp-7-4419-2007, 2007.

991 Price, C., Penner, J. and Prather, M.: NOx from lightning, Part I: Global distribution based on
992 lightning physics, J. Geophys. Res. Atmos., 102, D5, DOI: 10.1029/96JD03504, 1997.

993 Sindelarova, K., Granier, C., Bouarar, I., Guenther, A., Tilmes, S., Stavrakou, T., Müller, J.-F.,

994 Kuhn, U., Stefani, P., and Knorr, W.: Global dataset of biogenic VOC emissions calculated by
995 the MEGAN model over the last 30 years, Atmos. Chem. Phys. Discuss., 14, 10725-10788,
996 doi:10.5194/acpd-14-10725-2014, 2014.

997 Streets, D. G., Bond, T. C., Carmichael, G. R., Fernandes, S. D., Fu, Q., He, D., Klimont, Z.,
998 Nelson, S. M., Tsai, N. Y., Wang, M. Q., Woo, J.-H., and Yarber, K. F.: An inventory of
999 gaseous and primary aerosol emissions in Asia in the year 2000, J. Geophys. Res., 108, 8809,
1000 doi:10.1029/2002JD003093, 2003.

1001 Street, D. G., Fu, J. S., Jang, C. J., Hao, J. M., He, K. B., Tang, X. Y., Zhang, Y. H., Wang, Z.
1002 F., Li, Z. P., Zhang, Q., Wang, L. T., Wang, B. Y., Yu, C.: Air quality during the 2008
1003 Beijing Olympic Games, Atmos. Environ.,41, 480-492, 2007.

1004 Tang, X. L., Zhang, Y., Yi, H. H., Ma J. Y., Pu L.: Development a detailed inventory
1005 framework for estimating major pollutants emissions inventory for Yunnan Province, China,
1006 Atmos. Environ., 57, 116-125, 2012.

1007 Tian, H. Z., Liu, K. Y., Hao, J. M., Wang, Y., Gao, J. J., Qiu, P. P., and Zhu, C. Y.: Nitrogen
1008 oxides emissions from thermal power plants in China: Current status and future predictions,
1009 Environ. Sci. Technol., 47, 11350-11357, 2013.

1010 Wang, K., Zhang, Y., Jang, C., Phillip, S., and Wang, B.Y.: Modeling intercontinental air
1011 pollution transport over the trans-Pacific region in 2001 using the Community Multi scale Air
1012 Quality modeling system, J. Geophys. Res. Atmos., 114, D04307,
1013 doi:10.1029/2008JD010807, 2009.

1014 Wang, Q. D., Huo, H., He, K. B., Yao, Z. L., Zhang, Q.: Characterization of vehicle driving
1015 patterns and development of driving cycles in Chinese cities, Transportation research part D:
1016 transport and environment, 13, 289-297, 2008.

1017 Wang, S. X., Zhao, M., Xing, J., Wu, Y., Zhou, Y., Lei, Y., He, K. B., Fu, L. X., and Hao, J.
1018 M.: Quantifying the air pollutants emission reduction during the 2008 Olympic Games in
1019 Beijing, Environ. Sci. Technol., 44, 2490-2496, 2010.

1020 Wang, S. X., Xing, J., Jang, C. J., Zhu, Y., Fu, J. S., Hao, J. M.: Impact assessment of
1021 ammonia emissions on inorganic aerosols in east China using response surface modeling
1022 technique, Environ. Sci. Technol., 45: 9293-9300, 2011.

1023 Wang, L. T., Jang, C., Zhang, Y., Wang, K., Zhang, Q., Streets, D. G., Fu, C. J., Lei, Y.,
1024 Schreifels, J., He, K. B., Hao, J. M., Lam, Y. F., Lin, J., Meskhidze, N., Voorhees S., Evarts
1025 D., Phillips S.: Assessment of air quality benefits from national air pollution control policies
1026 in China. Part II: Evaluation of air quality predictions and air quality benefits assessment.
1027 Atmos. Environ., 44, 3449-3457, 2010.

1028 Wang, L. T., Wei, Z., Yang, J., Zhang, Y., Zhang, F. F., Su, J., Meng, C. C., and Zhang, Q.:
1029 The 2013 severe haze over southern Hebei, China: model evaluation, source apportionment,
1030 and policy implications, Atmos. Chem. Phys., 14, 3151–3173, doi:10.5194/acp-14-3151-2014,
1031 2014.

1032 Wei, W., Wang, S. X., Chatani, S., Klimont, Z., Cofala, J., and Hao, J. M.: Emission and

speciation of non-methane volatile organic compounds from anthropogenic sources in China, Atmos. Environ., 42, 4976–4988, 2008.

Xia, S. J., Zhao, Q. Y., Li, B., Shen, G. F.: Anthropogenic source VOCs emission inventory of Jiangsu Province, Research of Environmental Sciences, 27, 120-126, 2014 (in Chinese).

Xia, Y. M., Zhao, Y., Nielsen, C. P.: The benefits of China's efforts in gaseous pollutant control indicated by the bottom-up emissions and satellite observations, Atmos. Environ., 136, 43-53, 2016.

Xing, J., Zhang, Y., Wang, S. X., Liu, X. H., Cheng, S. H., Zhang, Q., Chen, Y. S., Streets, D. G., Jang, C. J., Hao, J. M., Wang, W. X.: Modeling study on the air quality impacts from emission reductions and a typical meteorological conditions during the 2008 Beijing Olympics, Atmos. Environ., 45, 1786-1798, 2011.

Yang, F., Tan, J., Zhao, Q., Du Z., He, K., Ma, Y., Duan, F., Chen, G., and Zhao, Q.: Characteristics of $PM_{2.5}$ speciation in representative megacities and across China, Atmos. Chem. Phys., 11, 5207-5219, doi:10.5194/acp-11-5207-2011, 2011.

Ye, S. Q., Zheng, J. Y., Pan, Y. Y., Wang, S. S., Lu, Q., and Zhong, L. J.: Marine emission inventory and its temporal and spatial characteristics in Guangdong Province, Acta Sci. Circum., 34, 537–547, 2014 (in Chinese).

Yin, S. S., Zheng, J. Y., Zhang, L. J., and Zhong, L. J.: Anthropogenic ammonia emission inventory and characteristic in the Pearl River Delta region, Environ. Sci., 31, 1146–1151, 2010 (in Chinese).

Yin, S. S., Zheng, J. Y., Lu, Q., Yuan, Z. B., Huang, Z. J., Zhong, L. J., Lin, H.: A refined 2010-based VOC emission inventory and its improvement on modeling regional ozone in the Pearl River Delta Region, China, Sci. Total Environ., 514, 426-438, 2015.

Zhang, H. L., Li, J. Y., Ying, Q., Yu, J. Z., Wu, D., Cheng, Y., He, K. B., Jiang, J. K.: Source apportionment of $PM_{2.5}$ nitrate and sulfate in China using a source-oriented chemical transport model, Atmos. Environ., 62, 228-242, 2012.

Zhang, L. J., Zheng, J. Y., Yin, S. S., Peng, K., and Zhong, L. J.: Development of non-road mobile source emission inventory for the Pearl River Delta region, Environ. Sci., 31, 886-891, 2010 (in Chinese).

Zhang, Q., Streets, D. G., Carmichael, G. R., He, K., Huo, H., Kannari, A., Klimont, Z., Park, I., Reddy, S., Fu, J. S., Chen, D., Duan, L., Lei, Y., Wang, L., and Yao, Z.: Asian emissions in 2006 for the NASA INTEX-B mission, Atmos. Chem. Phys., 9, 5131-5153, doi:10.5194/acp-9-5131-2009, 2009.

Zhang, Y. and Carmichael, G. R.: The role of mineral aerosol in tropospheric chemistry in East Asia-a model study, J. Appl. Meteorol., 38, 353-366, 1999.

Zhang, Y., Liu, P., Pun, B., Seigneur, C.: A comprehensive performance evaluation of MM5-CMAQ for the Summer 1999 Southern Oxidants Study episode-Part I: Evaluation protocols, databases, and meteorological predictions, Atmos. Environ., 40, 4825-4838, 2006.

Zhang, Y., Wang, W., Wu, S.-Y. Wang, K., Minoura, H., Wang, Z. F.: Impacts of updated emission inventories on source apportionment of fine particle and ozone over the southeastern U.S., Atmos. Environ., 88, 133-154, 2014.

Zhao, B., Wang, P., Ma, J. Z., Zhu, S., Pozzer, A., and Li, W.: A high-resolution emission inventory of primary pollutants for the Huabei region, China, Atmos. Chem. Phys., 12, 481-501, doi:10.5194/acp-12-481-2012, 2012.

Zhao, B., Wang, S. X., Dong, X. Y., Wang, J. D., Duan, L., Fu, X., Hao, J. M., and Fu, J. S.: Environmental effects of the recent emission changes in China: implications for particulate matter pollution and soil acidification, Environ. Res. Lett., 8, 24-31, 2013.

Zhao, Y., Wang, S.X., Duan, L., Lei, Y., Cao, P.F., and Hao, J.M.: Primary air pollutant emissions of coal-fired power plants in China: current status and future prediction. Atmos. Environ., 42, 8442-8452, 2008.

Zhao, Y., Wang, S. X., Nielsen, C. P., Li, X. H., and Hao, J. M.: Establishment of a database of emission factors for atmospheric pollutants from Chinese coal-fired power plants, Atmos. Environ., 44, 1515-1523, 2010.

Zhao, Y., Nielsen, C. P., McElroy, M. B., Zhang, L., and Zhang, J.: CO emissions in China: uncertainties and implications of improved energy efficiency and emission control, Atmos. Environ., 49, 103-113, 2012a.

Zhao, Y., Nielsen, C. P., and McElroy, M. B.: China's CO_2 emissions estimated from the bottom up: Recent trends, spatial distributions, and quantification of uncertainties, Atmos. Environ., 59, 214-223, 2012b.

Zhao, Y., Zhang, J., Nielsen, C. P.: The effects of recent control policies on trends in emissions of anthropogenic atmospheric pollutants and CO_2 in China, Atmos. Chem. Phys., 13, 487-508, 2013.

Zhao, Y., Qiu, L. P., Xu, R. Y., Xie, F. J., Zhang, Q., Yu, Y. Y., Nielsen, C. P., Qin, H. X., Wang, H. K., Wu, X. C., Li, W. Q., and Zhang, J.: Advantages of a city-scale emission inventory for urban air quality research and policy: the case of Nanjing, a typical industrial city in the Yangtze River Delta, China, Atmos. Chem. Phys., 15, 12623-12644, doi:10.5194/acp-15-12623-2015, 2015.

Zhao, Y., Mao, P., Zhou, Y., Yang, Y., Zhang, J., Wang, S., Dong, Y., Xie, F., Yu, Y., and Li, W.: Improved provincial emission inventory and speciation profiles of anthropogenic non-methane volatile organic compounds: a case study for Jiangsu, China, in preparation.

Zheng, J. Y., Zhang, L. J., Che, W. W., Zheng, Z., and Yin, S. S.: A highly resolved temporal and spatial air pollutant emission inventory for the Pearl River Delta region, China and its uncertainty assessment, Atmos. Environ., 43, 5112–5122, 2009.

Zheng, J. Y., Fu, F., Li, Z. C., Wang, S. S., Zhong, L. J.: Implementation and evaluation of uncertainty propagation using stochastic response surface method based on the CMAQ model, Acta Sci. Circum., 32, 1289-1298, 2012 (in Chinese).

FIGURE CAPTIONS

Figure 1. Modeling domain and locations of 43 meteorological and 9 air quality monitoring sites.

Figure 2. Source contributions to total estimated emissions by species in Jiangsu 2012. Colors indicate the sectors and the shade patterns indicate the source type (point, mobile and area).

Figure 3. Comparison between the emissions estimated in this work and other studies for Jiangsu. A and B indicate the emissions without and with open biomass burning, respectively.

Figure 4. Spatial distributions (a-c) and linear regression (d) of certain pollutant emissions from typical sources estimated in our provincial inventory and MEIC. (a) SO_2 from power plant; (b) NOx from transportation; (c) $PM_{2.5}$ from industry. The black points indicate the locations of plants with $PM_{2.5}$ emissions larger than 10 Gg estimated in this work.

Figure 5. Spatial distributions of NO_2 VCDs observed by OMI in Jiangsu in 2010 (a) and 2012 (b), and those of Jiangsu's NOx emissions from MEIC (c) and our provincial inventory (d) at the resolution of $0.25^{\circ}\times0.25^{\circ}$. Linear regressions of gridded VCDs and emissions are illustrated for MEIC (e) and our provincial inventory (f).

Figure 6. Spatial distributions of the monthly means of simulated SO_2, NO_2, $PM_{2.5}$ and O_3 concentrations using the national, regional and provincial emission inventories for October 2012.

Figure 7. The differences in the monthly means of simulated SO_2, NO_2, $PM_{2.5}$ and O_3 concentrations using different emission inventories: (a) Provincial–national; (b) Regional–national; and (c) provincial–regional. The black star A and triangle B referred to the locations of grids with maximum SO_2 emissions in provincial and regional inventory.

Figure 8. The observed and simulated hourly SO_2 concentrations (expressed with 3-h interval) using the national, regional, and provincial inventories at XWH (a), RJL (b), and ZHM (c) from October 6^{th} to 13^{th}, 2012.

Figure 9. Spatial distributions of the estimated SO_2 emissions in Nanjing at the resolution of 3×3km in the provincial (a), regional (b) and national emission inventory (c). The black dots indicate the locations of given air quality monitoring sites. The black star (point A) indicates the location of the power plant with the largest SO_2 emissions estimated in the provincial inventory. The black triangle (point B) indicates the speculated position of the same power plant in the regional inventory.

Figure 10. The changes in simulated O_3 concentrations at urban (XWH, SXL, RJL, MGQ, ZHM, and CCM) and suburban air quality monitoring sites (XLS, OSC, and PKS) in Nanjing under P1 (a) and P2 (b) scenarios compared to the base case for 6^{th}-16^{th} October 2012.

TABLES

Table 1. The estimated annual emissions by city for Jiangsu 2012 (unit: million metric tons (Tg) for CO_2 and kilo metric tons (Gg) for other species).

City	SO_2	NOx	CO	TSP	PM_{10}	$PM_{2.5}$	BC	OC	CO_2	NH_3	VOCs
Southern											
Nanjing	140.6	210.5	742.9	157.3	97.3	75.8	5.8	7.1	97.1	64.2	221.9
Suzhou	220.8	286.7	1383.3	380.6	194.9	137.3	9.8	11.0	184.4	144.8	297.8
Wuxi	107.7	180.0	545.5	271.3	126.9	77.2	3.4	9.6	84.5	24.2	167.2
Changzhou	104.0	107.7	734.6	413.3	194.6	126.2	3.6	7.5	65.2	33.4	104.2
Zhenjiang	44.0	89.6	231.6	143.3	66.8	40.9	1.9	6.6	53.0	38.1	55.4
Central											
Nantong	76.8	130.1	443.4	244.9	108.2	66.0	4.8	9.3	51.6	181.7	162.2
Yangzhou	55.3	93.9	310.7	54.1	39.9	31.1	2.6	8.5	52.1	83.1	82.5
Taizhou	56.6	70.5	315.1	207.6	98.2	52.3	2.7	8.8	31.4	100.7	76.9
Northen											
Xuzhou	138.9	232.5	805.5	223.2	146.5	101.9	6.1	19.1	139.2	49.2	161.2
Huai'an	52.2	61.5	590.0	97.4	64.5	49.5	3.7	12.0	32.5	195.9	78.6
Yancheng	49.9	78.5	639.7	203.8	111.8	72.0	5.6	16.1	28.2	101.0	185.0
Lianyungang	60.6	61.0	571.1	131.0	89.0	68.6	3.9	11.9	28.3	25.1	78.0
Suqian	34.1	39.7	366.8	77.8	55.5	42.3	3.2	11.0	12.9	59.1	76.4
Total	1141.5	1642.2	7680.0	2605.6	1394.0	941.1	57.0	138.5	860.5	1100.3	1747.3

Table 2. Model performance statistics for concentrations of given species from observation and CMAQ simulation using the national, regional and provincial inventories at the nine air quality monitoring sites in Nanjing for October 2012.

Pollutants	National (MEIC)		Regional (Fu et al., 2013)		Provincial (this work)	
	NMB	NME	NMB	NME	NMB	NME
SO_2	48.45%	76.53%	74.08%	95.04%	-9.97%	47.49%
NO_2	21.02%	35.99%	29.84%	43.45%	-14.47%	33.22%
O_3	-65.55%	68.57%	-53.93%	61.59%	-24.98%	44.29%
$PM_{2.5}$	-51.63%	55.32%	-49.16%	56.00%	-43.64%	51.81%

Note: NMB and NME were calculated using following equations (*P* and *O* indicate the results from modeling prediction and observation, respectively):

$$NMB = \frac{\sum_{i=1}^{n}(P_i - O_i)}{\sum_{i=1}^{n} O_i} \times 100\%; \quad NME = \frac{\sum_{i=1}^{n}|P_i - O_i|}{\sum_{i=1}^{n} O_i} \times 100\%$$

Table 3. The annual SO_2 emissions estimated in three inventories at given air quality monitoring sites in downtown Nanjing.

SO_2/Mg	National (MEIC)	Regional (Fu et al., 2013)	Provincial (this work)
XWH	1297.5	1790.9	411.0
RJL	1297.5	1720.8	303.1
ZHM	1297.5	1918.3	396.2
CCM	928.6	1635.3	371.8
MGQ	1297.5	478.6	395.0

Table 4. The monthly mean contributions of power, iron & steel and cement plants to the $PM_{2.5}$ concentrations at the air quality monitoring sites in Nanjing in October 2012.

Monitoring site	Contri. of power (%)			Contri. of iron & steel (%)			Contri. of cement (%)		
	Max.	Min.	Ave.	Max.	Min.	Ave.	Max.	Min.	Ave.
XWH/SXL	52	-6	8	82	-2	14	43	-1	8
RJL	42	-6	7	79	0	11	44	0	9
ZHM	44	-5	7	71	-3	12	48	0	9
CCM	32	-8	7	83	-4	13	58	-5	8
MGQ	58	-5	9	89	-2	8	35	-5	7
XLS	35	-5	7	67	-3	10	57	0	10
PKS	65	-6	7	77	-1	11	45	-1	7
OCS	33	-7	7	87	0	12	58	0	8

Note: Max., min., ave. and contri. indicate maximum, minimum, average and contribution, respectively.

Figure 1

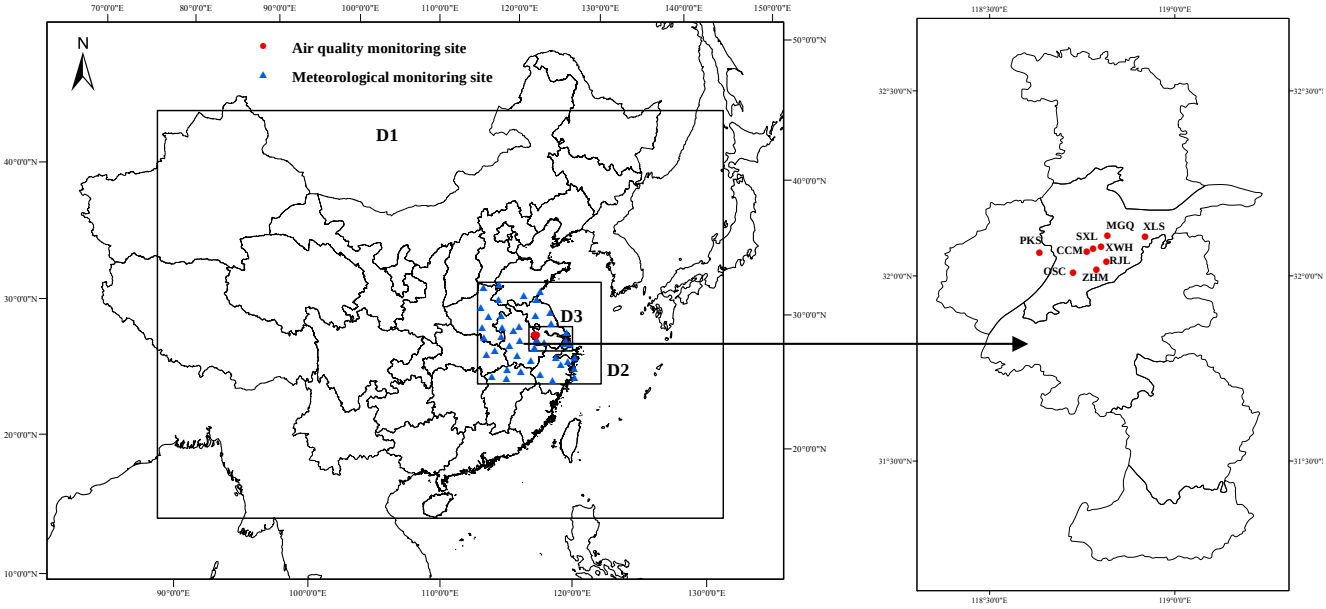
N
Air quality monitoring site
Meteorological monitoring site
D1
D2
D3
PKS
SXL
MGQ
XLS
CCM
XWH
RJL
QSC
ZHM

Figure 2

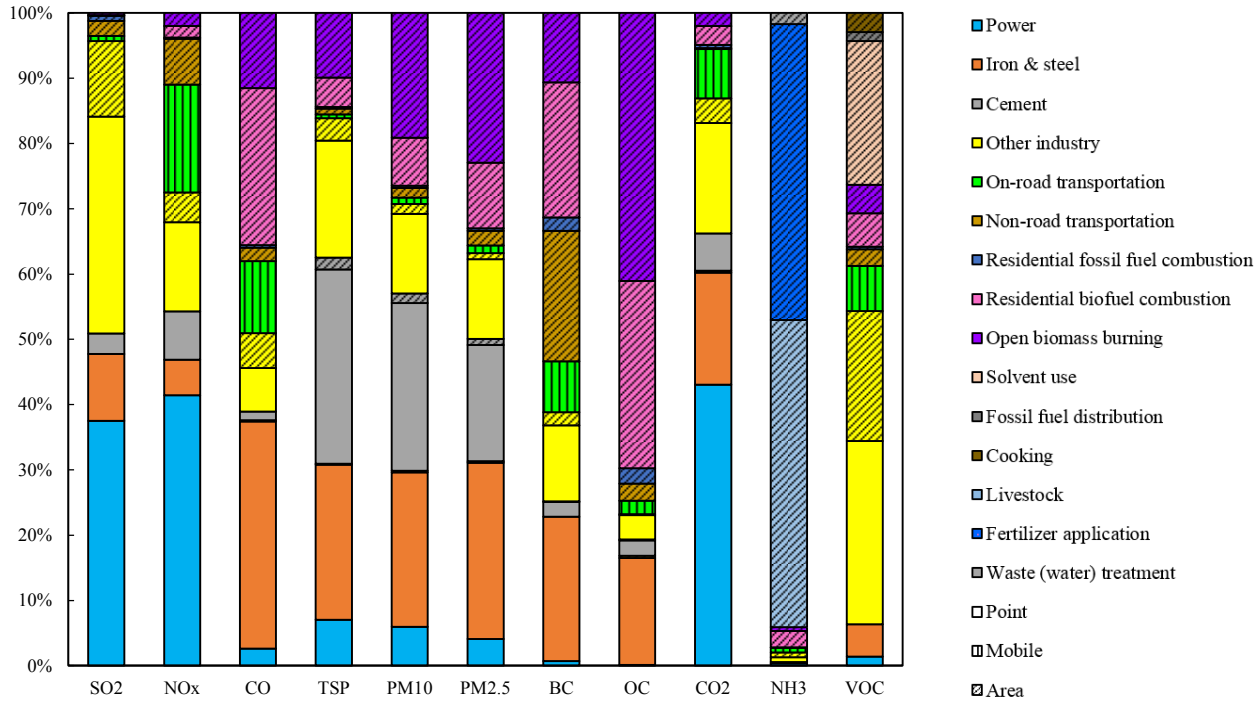
100%
90%
80%
70%
60%
50%
40%
30%
20%
10%
0%
SO2
NOx
CO
TSP
PM10
PM2.5
BC
OC
CO2
NH3
VOC
Power
Iron & steel
Cement
Other industry
On-road transportation
Non-road transportation
Residential fossil fuel combustion
Residential biofuel combustion
Open biomass burning
Solvent use
Fossil fuel distribution
Cooking
Livestock
Fertilizer application
Waste (water) treatment
Point
Mobile
Area

Figure 3

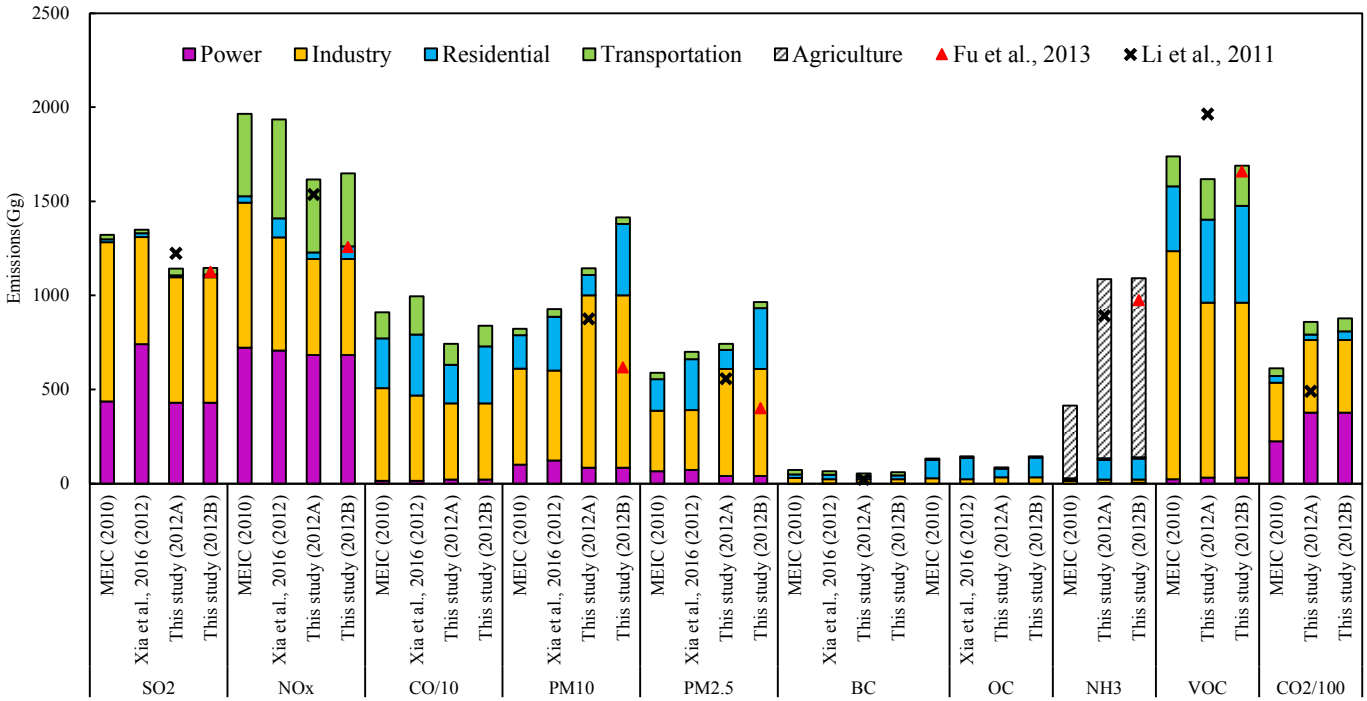
2500
2000
1500
1000
500
0
Emissions(Gg)
Power
Industry
Residential
Transportation
Agriculture
Fu et al., 2013
Li et al., 2011
MEIC (2010)
Xia et al., 2016 (2012)
This study (2012A)
This study (2012B)
SO2
NOx
CO/10
PM10
PM2.5
BC
OC
NH3
VOC
CO2/100

Figure 4

(a)

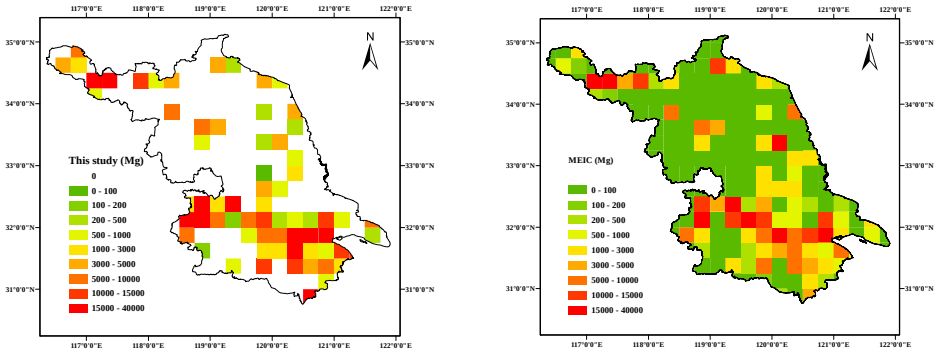

(b)

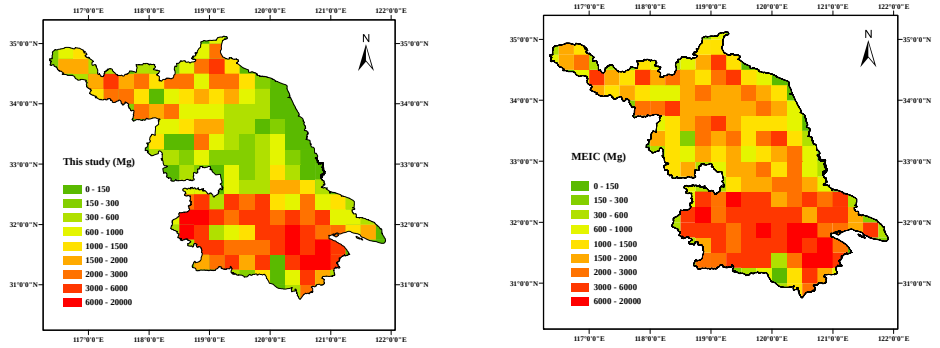

(c)

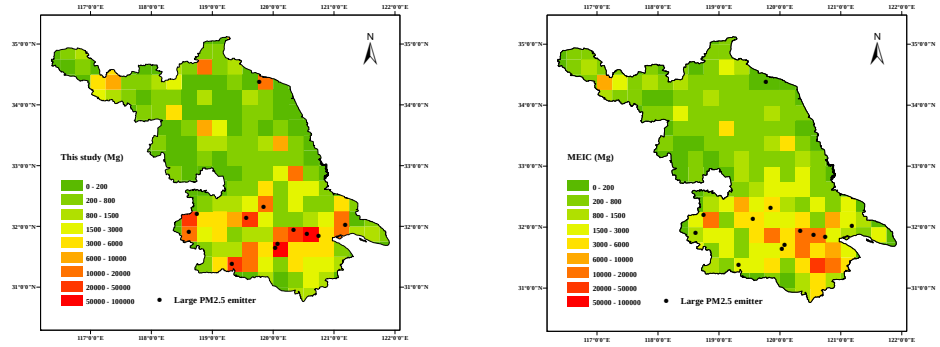

(d)

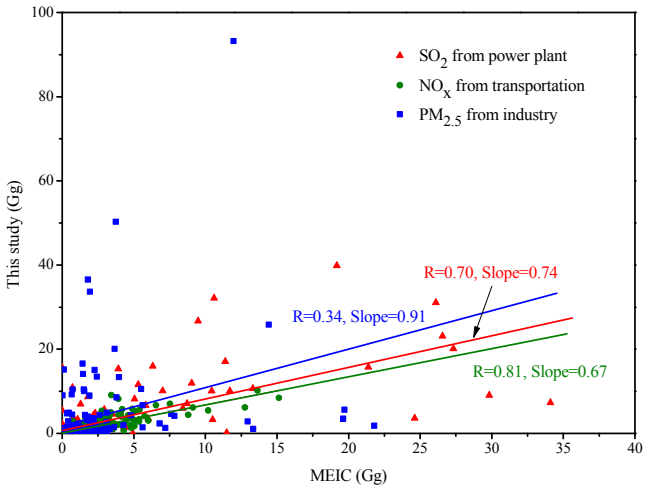

Figure 5

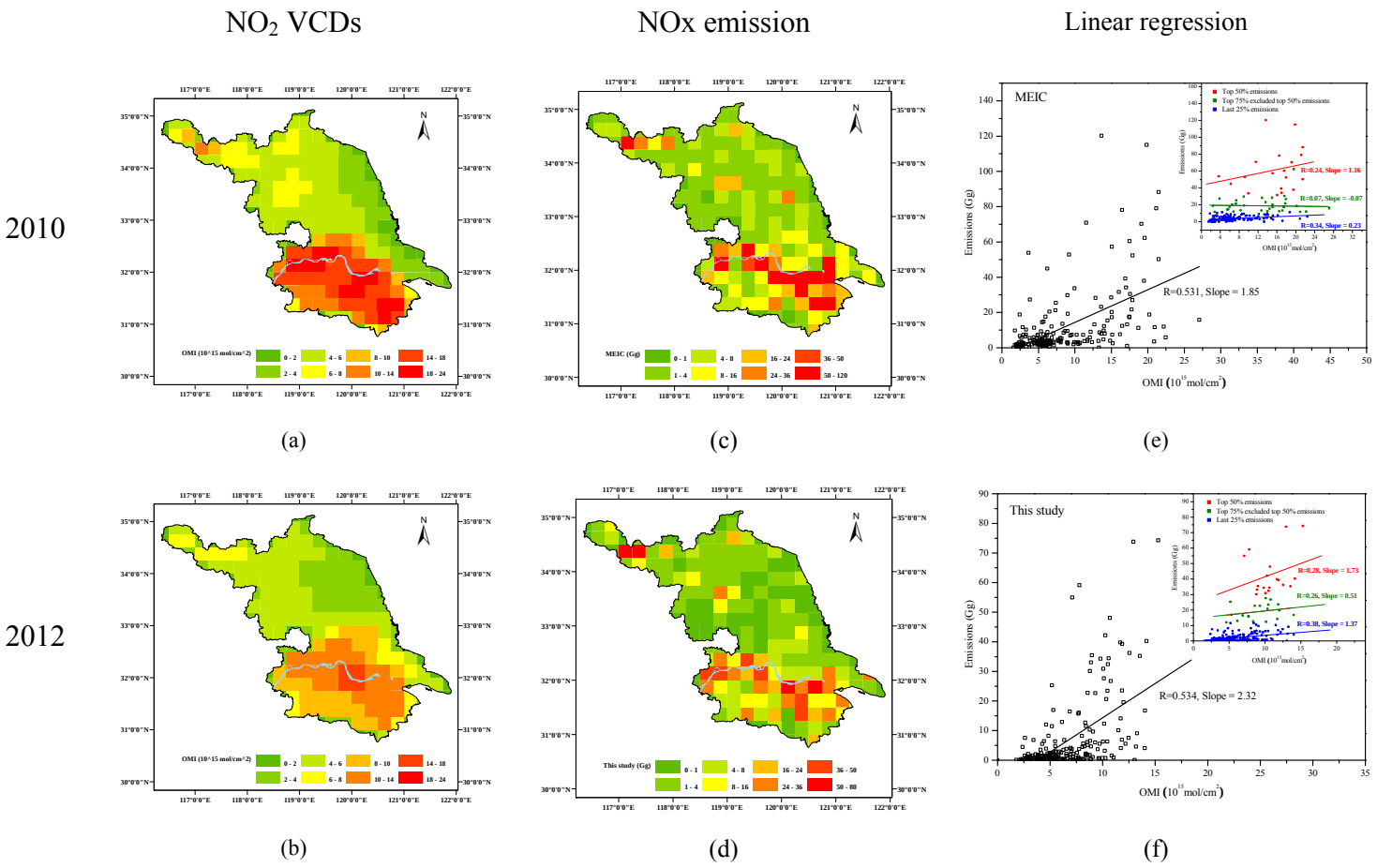
NO2 VCDs
NOx emission
Linear regression
2010
2012
MEIC
This study
R=0.531, Slope = 1.85
R=0.534, Slope = 2.32
Emissions (Gg)
OMI (10^15 mol/cm^2)
(a)
(b)
(c)
(d)
(e)
(f)

Figure 6

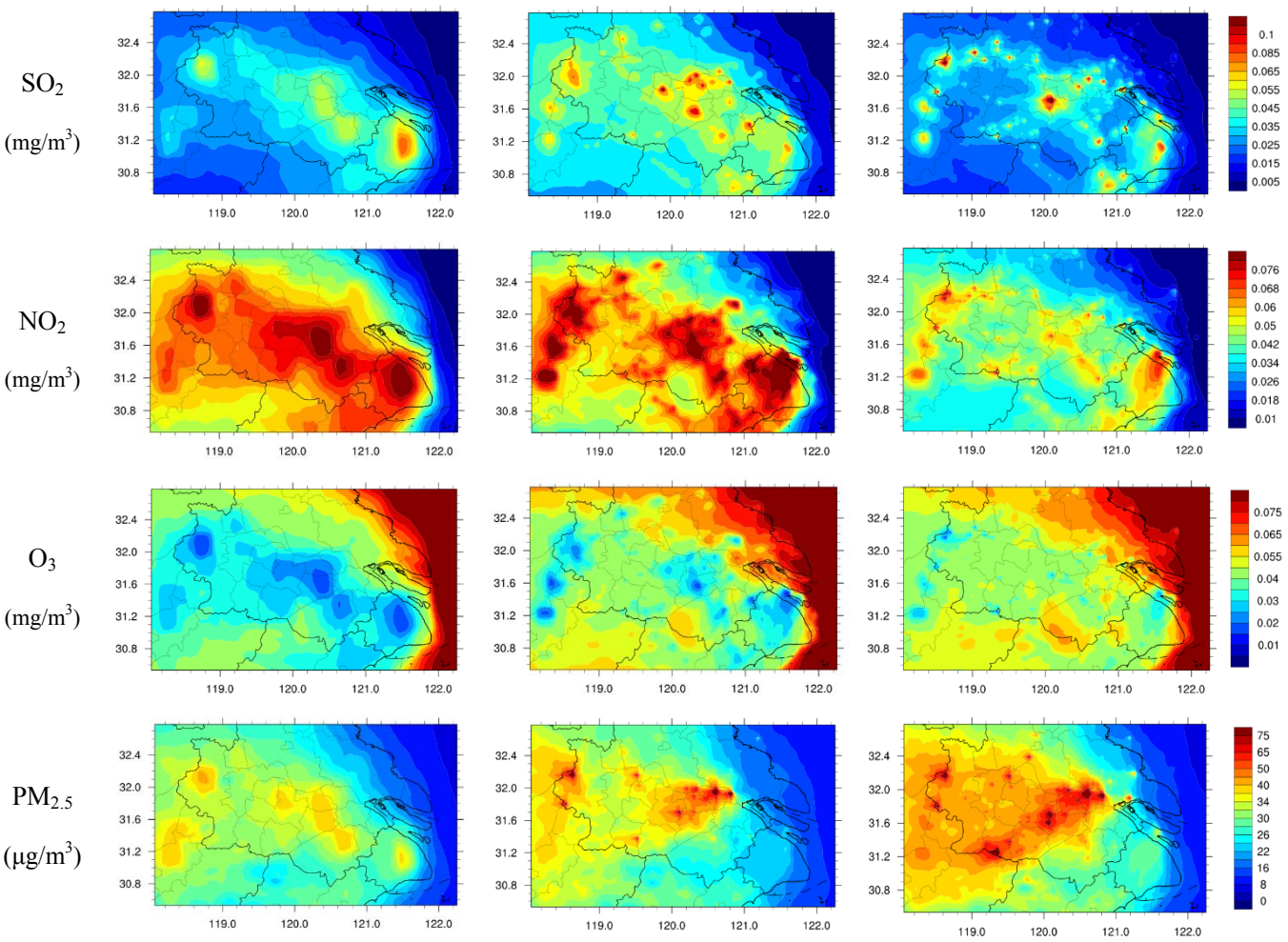

(a) National (MEIC) (b) Regional (Fu et al., 2013) (c) Provincial (this work)

Figure 7

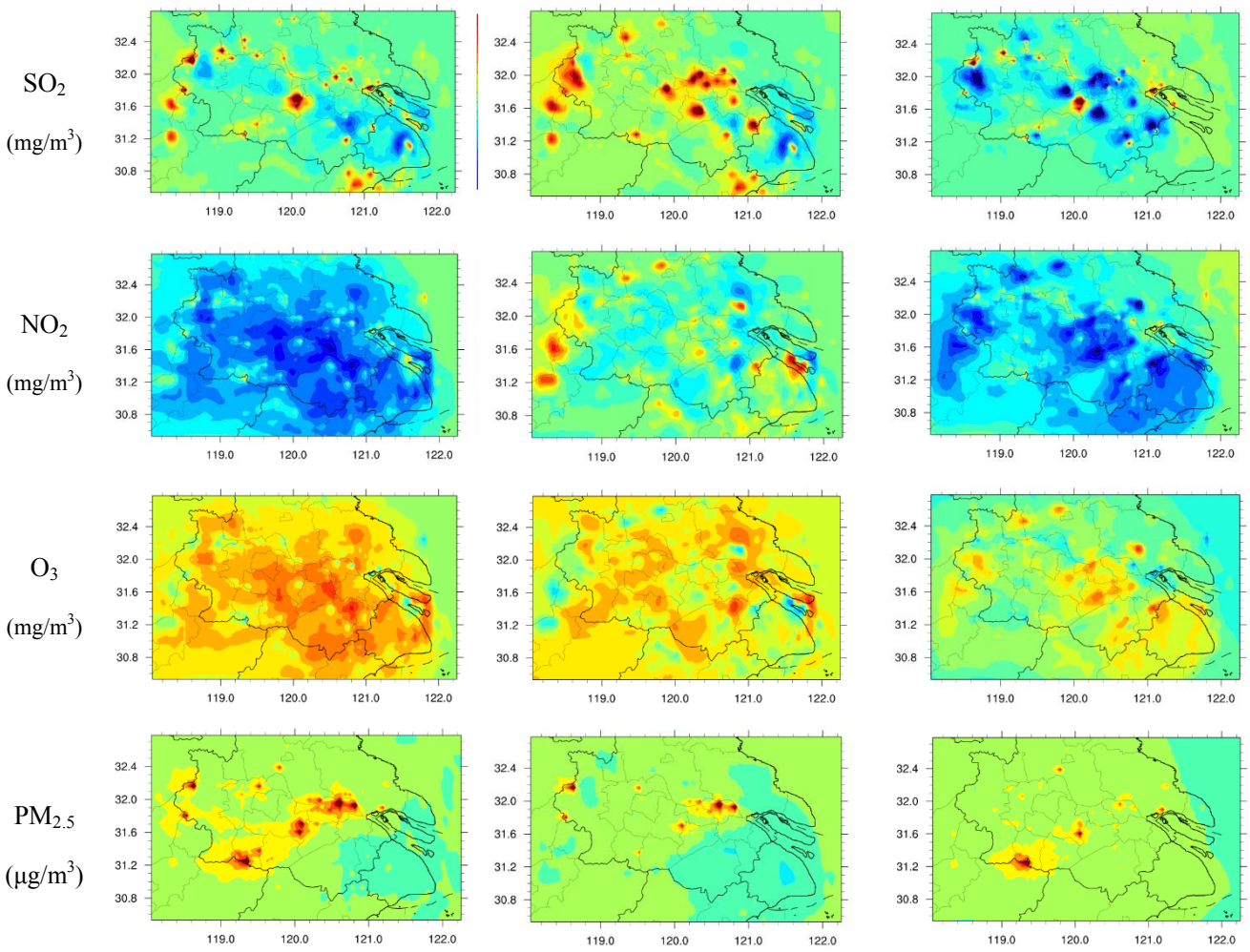

(a) Provincial – national (b) Regional – national (c) Provincial – regional

Figure 8

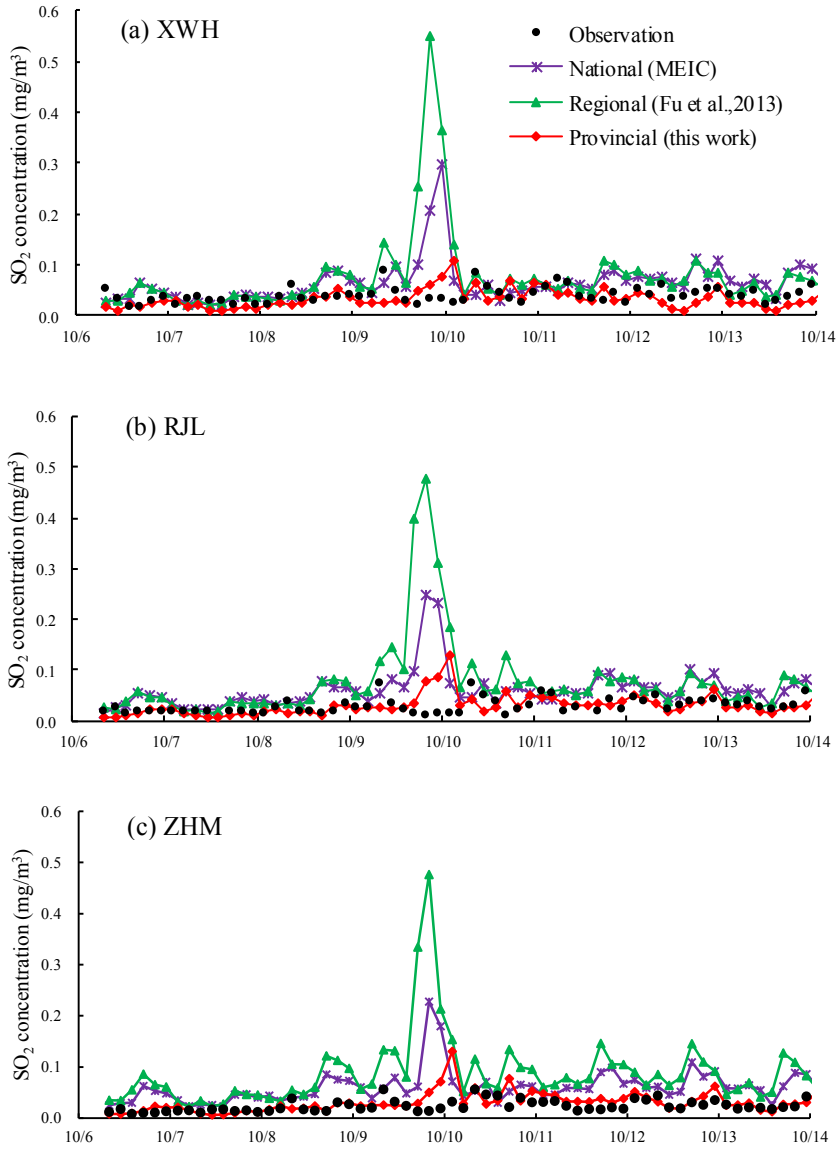
(a) XWH
Observation
National (MEIC)
Regional (Fu et al.,2013)
Provincial (this work)
SO2 concentration (mg/m3)
0.0
0.1
0.2
0.3
0.4
0.5
0.6
10/6
10/7
10/8
10/9
10/10
10/11
10/12
10/13
10/14
(b) RJL
SO2 concentration (mg/m3)
(c) ZHM
SO2 concentration (mg/m3)

Figure 9

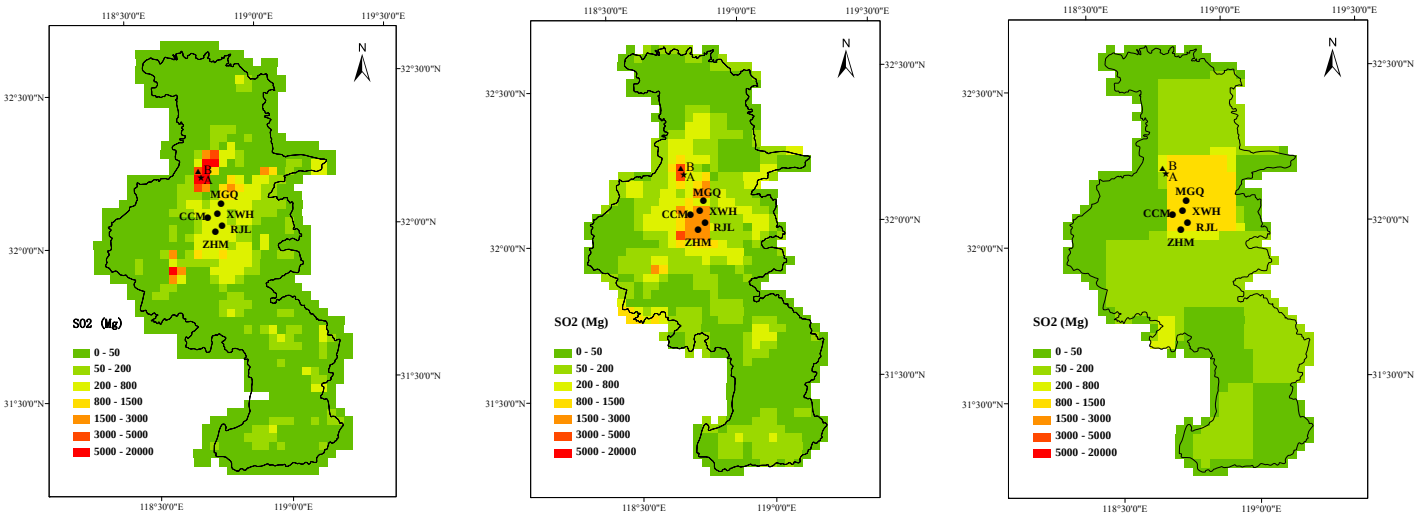
118°30'0"E
119°0'0"E
119°30'0"E
32°30'0"N
32°0'0"N
31°30'0"N
N
A
B
MGQ
CCM
XWH
RJL
ZHM
SO2 (Mg)
0 - 50
50 - 200
200 - 800
800 - 1500
1500 - 3000
3000 - 5000
5000 - 20000

(a) (b) (c)

Figure 10

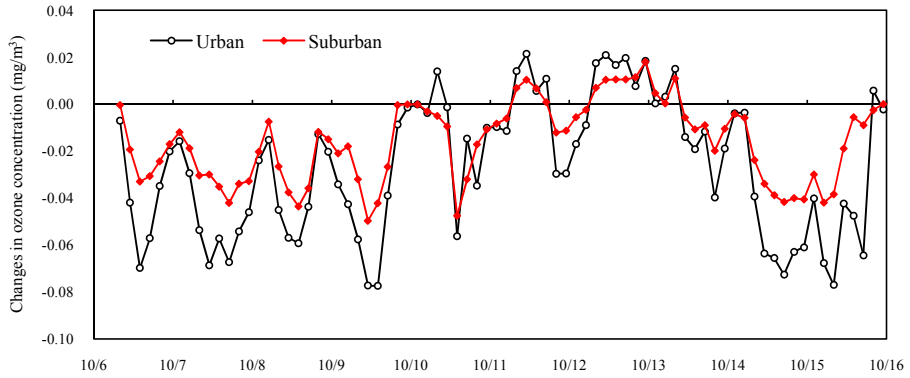
Urban
Suburban
Changes in ozone concentration (mg/m³)
0.04
0.02
0.00
-0.02
-0.04
-0.06
-0.08
-0.10
10/6
10/7
10/8
10/9
10/10
10/11
10/12
10/13
10/14
10/15
10/16

(a)

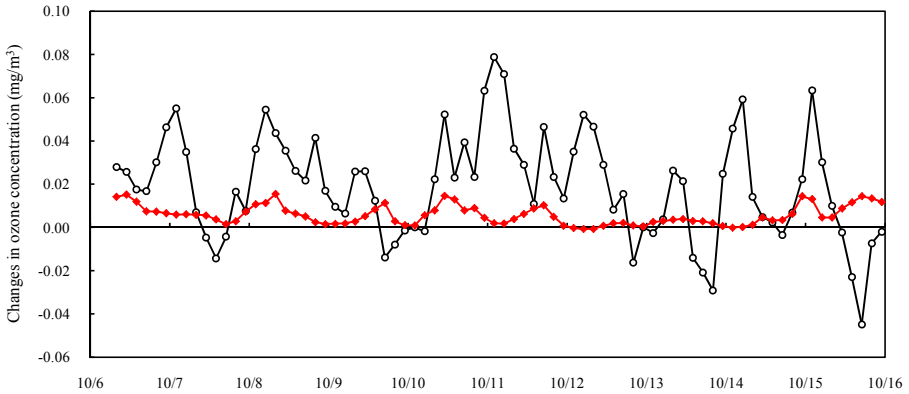
Changes in ozone concentration (mg/m³)
0.10
0.08
0.06
0.04
0.02
0.00
-0.02
-0.04
-0.06
10/6
10/7
10/8
10/9
10/10
10/11
10/12
10/13
10/14
10/15
10/16

(b)